Astrocytes promote a protective immune response to brain *Toxoplasma gondii* infection via IL-33-ST2 signaling

Katherine M. Still*, Samantha J. Batista*, Carleigh O'Brien*, Oyebola O. Oyesola**, Simon P. Früh**, Lauren M. Webb***, Igor Smirnov*, Michael A. Kovacs*, Maureen N. Cowan*, Nikolas W. Hayes*, Jeremy A. Thompson*, Elia D. Tait-Wojno***, and Tajie H. Harris*

Affiliations: *Center for Brain Immunology and Glia, Department of Neuroscience, University of Virginia

** Baker Institute for Animal Health and Department of Microbiology and Immunology, Cornell University; Department of Immunology, University of Washington

***Department of Immunology, University of Washington

Corresponding Author:

Tajie H. Harris, MR-4 Room 6148, 409 Lane Road, Charlottesville, VA 22908

Phone: 434-982-6916

Fax: 434-982-4380

Email: tajieharris@virginia.edu

This work was funded by a National Institutes of Health grants R01NS091067 and R01NS112516 to T. H H.; T32GM008328 to K. M. S. and J. A. T.; T32AI007046 to S. J. B.; T32AI007496 to C.A. O., M.N.C., and M.A.K.; T32GM007267 to M.A.K.; R01AI32708 and R01AI130379 grants to E.D.T.W; and a University of Virginia School of Medicine R&D grant.

SUMMARY

Understanding how invading pathogens are sensed within the brain is necessary to uncover how effective immune response are mounted in immunoprivileged sites. The eukaryotic parasite *Toxoplasma gondii* colonizes the brain of its hosts and initiates robust immune cell recruitment, but little is known about innate recognition of *T. gondii* within brain tissue. The host damage signal IL-33 is one protein that has been implicated in control of chronic *T. gondii* infection, but the specific impact of IL-33 signaling within the brain is unclear. Here, we show that IL-33 is expressed by oligodendrocytes and astrocytes during *T. gondii* infection, is released into the cerebrospinal fluid of *T. gondii*-infected animals, and is required for control of infection. IL-33 signaling promotes chemokine expression within brain tissue and is required for the recruitment of peripheral anti-parasitic immune cells, including IFN-γ-expressing T cells and iNOS-expressing monocytes. Importantly, we find that the beneficial effects of IL-33 during chronic infection are not a result of signaling on infiltrating immune cells, but rather on radio-resistant responders, and specifically, astrocytes. Mice with IL-33R-deficient astrocytes fail to promote an adaptive immune response in the CNS and control parasite burden, demonstrating that astrocytes can directly respond to IL-33 *in vivo*. Together, these results indicate a brain-specific mechanism by which IL-33 is released and sensed locally, to engage the peripheral immune system in controlling a neurotropic pathogen.

54 **INTRODUCTION**

55

56 Recruitment of immune cells to the brain during infection is a highly orchestrated process,
57 requiring concerted expression of a number of chemokines and adhesion factors at the blood-
58 brain barrier[1]. But the cues which precede these factors are less well understood. In particular, in
59 many cases, it is unclear if brain resident cells possess the machinery to detect the presence of
60 pathogens to promote the recruitment of peripheral cells. Murine infection with the eukaryotic
61 parasite *Toxoplasma gondii (T. gondii)* features continual recruitment of blood-derived immune
62 cells to the brain and serves as an excellent model for better understanding immune responses
63 at this site.

64 *T. gondii* is a globally relevant pathogen which infects most warm-blooded vertebrates,
65 including one-third of the human population[2-4]. Upon initial infection, *T. gondii* disseminates
66 throughout peripheral tissues, where it is largely cleared, but ultimately persists in the brain of its
67 hosts for their lifetime[2,5-8]. Mortality from *T. gondii* infection is associated with an increased
68 prevalence of replicating parasite in brain tissue, documented in immunosuppressed patients
69 undergoing transplant surgeries[9], and in HIV-AIDS patients[10-12], highlighting the importance of the
70 immune response in controlling *T. gondii*. Indeed, control of brain *T. gondii* infection requires a
71 Th1-dominated immune response,[2,8] whereby CD4+ and CD8+ T cells and the IFN-γ they produce
72 are required for survival[13]. Macrophages also exhibit anti-parasitic effector mechanisms which are
73 necessary to control the parasite[8,14-20].

74 It is not known, however, how the parasite is sensed in the brain to create an environment
75 that promotes immune cell entry, stimulation, and maintenance. During the acute phase of
76 infection in the periphery, dendritic cells and macrophages can sense either the parasite itself or
77 host signals to initiate chemokine and cytokine expression which recruits and skews a strong Th1
78 immune response[8,21-25]. However, resident dendritic cells and peripheral immune cells do not exist
79 in brain tissue under steady-state conditions[26,27] and it is unclear if *T.gondii*-specific molecular

80 patterns are sensed in this tissue. During chronic *T. gondii* infection of the brain, necrotic lesions
81 form, characterized by the presence of replicating parasite, loss of brain-resident cell markers,
82 and infiltration of immune cells, suggestive of tissue damage and alarmin release[13,28-32]. We
83 hypothesized that indirect sensing of *T. gondii* infection, via recognition of host cell damage
84 caused by the parasite, is an important step in instructing the immune response to *T. gondii* in the
85 brain. Here we focused on the nuclear alarmin, IL-33, as a candidate orchestrator of the immune
86 response to *T. gondii*. IL-33 is highly expressed in brain tissue[33], and IL-33 signaling has been
87 shown to be protective against tissue pathology during chronic *T. gondii* infection, but the
88 mechanism by which IL-33 signals, and the immune mechanisms underlying this protection, were
89 not studied in detail[34].

90 IL-33 is categorized as an alarmin because it is known to amplify immune responses upon
91 signaling through its receptor ST2, without a requirement for secretion or cleavage. A role for IL-
92 33 in stroke[35,36], neurodegeneration[37,38], EAE[39,40], and CNS infection[41-43] has been described, but
93 mechanistic understanding of IL-33 signaling during brain disease is limited. It is unclear in many
94 instances which cell type(s) is the relevant responder to IL-33 during disease in the brain. While
95 brain-resident macrophages have been shown to express IL-33 receptor at baseline[44], astrocytes
96 have been shown to upregulate it during pathology[36,45]. In addition, IL-33 receptor is also
97 expressed on immune cells which can infiltrate the brain from the blood during disease[46,47]. Here,
98 we separate the relative contribution of astrocytes, microglia/macrophages, and infiltrating
99 immune cells in response to IL-33 release during brain pathology, finding that IL-33 can signal
100 strictly within the brain to promote protective immunity to *T. gondii*.

101
102
103

RESULTS

IL-33 is released during *T. gondii* brain infection and is required to control parasite

To study *T. gondii* brain infection, we infected mice by intra-peritoneal injection with the avirulent *T. gondii* strain Me49 and waited four weeks post infection for a natural, chronic brain infection to be established. At this timepoint, peripheral infection has been controlled[6,48]. For all experiments, brain tissue was harvested at four weeks post infection unless otherwise specified.

Consistent with its role as a pre-stored alarmin, IL-33 is expressed highly at baseline[33,44,45], and we detected only mild increases in IL-33 levels in infected versus uninfected tissue (Figure S1A). In the *T. gondii* infected brain parenchyma, we found nuclear IL-33 to be expressed by mature, CC1+ oligodendrocytes and by astrocytes, the percentages of which varied by brain region (Figures 1A, 1B, and S1B). While IL-33 was expressed almost exclusively by oligodendrocytes in white matter tracts, such as the corpus callosum, IL-33 expression in the cortex was split more evenly between astrocytes and oligodendrocytes (Figures 1A and 1B). Collectively, these results indicate that IL-33 is expressed by glia in the *T. gondii* infected mouse brain parenchyma. Importantly, we also detected IL-33 protein expression in astrocytes in healthy human brain tissue, as has been shown previously on the transcript level[49](Figures S1C and S1D).

Since IL-33 does not need to be cleaved to be active, it is classically thought of as an alarmin that is released by necrotic cell death. During *T. gondii* infection, the parasite itself as well as the inflammatory environment provide opportunity for host cell damage and alarmin release. *T. gondii* predominantly exists in the brain as an intracellular cyst form which is slow growing[7,48] (Figure 1C) and does not appear to pose an immediate risk to cells, due to a lack of observed tissue destruction and inflammation surrounding cysts (Figure 1C). But, for reasons not fully understood, cysts can reactivate anywhere in the brain, releasing individual parasites previously contained within the cyst wall[7,29] (Figure 1C). Individual parasites can invade surrounding cells,

130 replicate, and either lyse the cell or form a new cyst[50]. The presence of individual replicating
131 parasites is correlated with morbidity in humans, and is thought to cause necrotic lesions in
132 immunocompromised patients[9-12]. Interestingly, we found clusters of immune cells, including T
133 cells and macrophages, surrounding individual replicating parasites but not *T. gondii* cysts
134 (Figures S2A, S2B, 1C). Therefore, we hypothesized that either lytic *T. gondii* replication[50] or local
135 inflammation can cause release of local damage signals, such as IL-33. Corroborating this
136 hypothesis, while IL-33 tiles evenly throughout uninfected brain tissue[45], we noted focal loss of
137 IL-33 staining, as well as oligodendrocyte and astrocyte markers, at sites of parasite replication
138 and release (Figures 1D, S2C-E).

139 In order to determine if IL-33 is released during brain *T. gondii* infection, we first utilized
140 an *ex-vivo* assay to measure extracellular IL-33 during infection. We processed uninfected (naïve)
141 and infected mouse brains down to a single cell suspension containing brain resident cells as well
142 as immune cells and parasite. We then incubated the single cell suspensions for four hours at
143 37°C before taking the supernatant and measuring extracellular IL-33 by ELISA. Strikingly, IL-33
144 was present in detectable quantities from supernatants of infected brain samples, but not naïve
145 controls, suggesting that *T. gondii* infection has the capacity to induce IL-33 release. We then
146 validated IL-33 release *in vivo*, by sampling CSF from the cisterna magna of infected mice and
147 found detectable IL-33 levels in pooled CSF samples (Figure 1F).

148 We next asked if IL-33 was required to control infection. We infected wildtype and IL-33$^{-/-}$
149 mice and assessed their brains for parasite burden, enumerating a significantly increased number
150 of cysts in IL-33-deficient mice (Figure 1G). We also detected an increased parasite burden in the
151 brains of infected IL-33 receptor (ST2) – deficient mice (Figure 1H), demonstrating a role for
152 extracellular IL-33 signaling during this infection. At day 10 post-infection, no parasite was
153 detected in the peritoneal cavity of infected ST2$^{-/-}$ or wildtype animals. Therefore, ST2$^{-/-}$ mice are
154 not delayed or defective in clearing parasite in the periphery. While neither IL-33$^{-/-}$ or ST2$^{-/-}$ mice

155 succumbed to infection, these results demonstrate that extracellular IL-33 signaling plays a role
156 in control of *T. gondii* brain infection.
157

158 **IL-33-ST2 signaling is required for adequate numbers of functional T cells during**
159 **chronic *T. gondii* infection.**

160 In order to better understand how IL-33 signaling was protective during *T. gondii* infection,
161 we focused on characterizing ST2$^{-/-}$ mice from this point onward. We first profiled recruited
162 immune cell populations in the brain, beginning with the adaptive immune response, because a
163 strong, Th1-biased immune response is absolutely critical for control of chronic *T. gondii*
164 infection[13]. In the absence of IL-33 signaling during infection, approximately one-third fewer total
165 T cells were present in the brain by flow cytometry (Figures 2A and 2B), suggesting an inability to
166 recruit or maintain these cells. Approximately 96% of T cells in *T. gondii* infected brains were
167 positive for either CD4 or CD8 markers (Figure 2A), and there was no selective decrease in either
168 of these subsets, but rather a general reduction in T cell counts in ST2$^{-/-}$ mice (Figures 2A and
169 2B). In addition to a reduction in T cells, T cell function was impaired in the absence of IL-33
170 signaling. Fewer CD4+ and CD8+ T cells were proliferating in the brain (Figures 2C and 2D), and
171 fewer of these cells were making the critical cytokine IFN-γ by *ex vivo* restimulation with
172 PMA/ionomycin (Figures 2E and 2F). IFN-γ is critical because it induces widespread anti-parasitic
173 changes, such as increasing chemokine production[51,52], adhesion factor expression[53], and
174 intracellular killing mechanisms of infected cell types, such as macrophages[8]. We found that the
175 chief sources of IFN-γ in the brain during our infection were CD4+ and CD8+ T cells, with minimal
176 contribution from NK cells, an important source of the cytokine during early stages of acute
177 infection[54](Figure S3A). These results show that extracellular IL-33 signaling is required to
178 maintain an adequate anti-parasitic T cell response in brain tissue. Importantly, T cell numbers
179 and function were unaffected at baseline in spleens of ST2$^{-/-}$ mice, in the spleen during chronic

180 infection, as well as at sites of inflammation such as the peritoneal cavity during acute infection
181 (Figure S3B-E). We did, however, note a decrease in T cell numbers in the blood during acute
182 infection of ST2$^{-/-}$ mice (Figure S3F).
183
184 **IL-33-ST2 signaling is required for the recruitment and anti-parasitic function of myeloid**
185 **cells during brain *T. gondii* infection.**
186 We were also interested in the impact of IL-33 signaling on the myeloid cell lineage since
187 macrophages cluster tightly around replicating parasite in brain tissue and express iNOS, a key
188 molecule invovled in the control of *T. gondii* (Figure S2B)[8]. We assessed numbers of CD11b+
189 myeloid cells in infected ST2$^{-/-}$ mice by flow cytometry, using CD45hi expression to differentiate
190 infiltrating myeloid cells from CD45int microglia (Figures 3A and 3B). Many of the CD45hi CD11b+
191 cells recruited to the *T. gondii*-infected brain are Ly6C+ CD11c- and Ly6G-, indicating that a large
192 portion of recruited myeloid cells are Ly6Chi monocytes and Ly6Clo monocyte-derived
193 macrophages[55]. Importantly, infected ST2$^{-/-}$ mice displayed a reduced frequency and number of
194 CD45hi myeloid cells, by approximately half, in the brain during chronic infection, while CD45int
195 cell numbers held constant (Figures 3A and 3B).
196 To more specifically assess monocyte recruitment, we used CCR2-RFP reporter mice to
197 visualize monocytes in the brain during chronic infection. Monocyte-derived cells are critical for
198 control of brain *T. gondii* infection, as anti-CCR2 antibody administered during chronic infection
199 results in rapid mortality[55]. By immunohistochemistry, we observed large numbers of CCR2+ cells
200 throughout the brain 4 weeks post infection in wildtype mice (Figure 3C). Importantly, we crossed
201 CCR2-reporters to a ST2$^{-/-}$ background, which revealed a marked reduction in CCR2+ cells
202 (Figures 3D and 3E). These results confirmed that there is a defect in monocyte recruitment in
203 the absence of IL-33 signaling during infection.
204 Next, we assessed the anti-parasitic function of the myeloid compartment in the absence
205 of IL-33 signaling. We focused on inducible nitric oxide synthase (iNOS) expression. Synthesis of

206 nitric oxide by host cells can deprive the parasite of essential amino acids and prevent parasite
207 growth *in vitro*[56]. *In vivo*, iNOS knockout mice succumb to infection during the early chronic
208 phase[15]. Of the myeloid cells that were able to infiltrate the brain, fewer of these cells were making
209 iNOS in the absence of IL-33 signaling (Figures 3F-I). Interestingly, we did not detect significant
210 iNOS positivity in any tissues, aside from the brain, in acute or chronic infection (Figure S4).
211 Additionally, no defects in myeloid cell number were found at baseline in uninfected $ST2^{-/-}$ mice,
212 in peripheral tissues during acute infection, including in the peritoneum, blood, and spleen, or in
213 peripheral tissues during chronic infection (Figure S4). In sum, these results, in conjunction with
214 T cell deficits, demonstrate that IL-33 signaling impacts the presence and function of immune cell
215 populations that are necessary for controlling *T. gondii* infection in the brain.
216
217 **IL-33-ST2 signaling induces expression of factors involved in recruitment of immune cells**
218 **to the brain**
219 Next, we sought to address how IL-33 is changing the environment within the brain to
220 make the tissue conducive to immune cell recruitment. Initiation and maintenance of an immune
221 response in the brain requires expression of cytokines, chemokines, adhesion factors, and factors
222 which promote the entry of and maintain proliferation of immune cells[1]. It is well known that *T.*
223 *gondii* infection induces many of these factors[51-53,57],which we validated by whole brain qRT-PCR.
224 We find a profound increase in brain *ccl2*, *cxcl9*, *cxcl10*, *ccl5*, *cxcl1*, *vcam*, and *icam* expression
225 over uninfected controls (Figure 4A). When we assessed the same genes in infected ST2-
226 deficient mice, we saw significantly decreased expression of the chemokines *ccl2*, *cxcl10*, and
227 *cxcl1* (Figure 4A), along with smaller reductions in the expression of the adhesion factors *vcam*
228 and *icam* (Figure 4B). Interestingly, *ccl2* and *cxcl10* expression has been attributed to astrocytes
229 by *in situ* hybridization during *T. gondii* infection[52]. Although *cxcl1* has not been extensively
230 studied in chronic *T. gondii* infection, it has also been reported in astrocytes during
231 neuroinflammation[58]. However, we did not observe an effect of IL-33 signaling on *cxcl9*

232 expression, a chemokine which is made by PU.1-expressing cells rather than astrocytes[59] (Figure
233 4B). These results suggest that IL-33 signaling, either directly or indirectly, could be inducing
234 chemokine expression in astrocytes during *T. gondii* infection.

235 We next wanted to identify the cellular source of chemokine in infected brain tissue to
236 better understand where IL-33 was exerting its effects. We focused on studying the expression
237 pattern of a chemokine whose transcript levels were altered to the greatest degree in the absence
238 of IL-33 signaling, the monocyte chemoattractant *ccl2*. We used immunofluorescence microscopy
239 to image the brain tissue of chronically infected *ccl2*-mCherry reporter mice[60]. We observed *ccl2*-
240 mCherry expression in "hotspots" throughout the brain, implicating a local response to signals in
241 brain tissue (Figure 4C). We validated by immunohistochemistry that *ccl2* expression was greatly
242 reduced in ST2$^{-/-}$ mice by crossing our *ccl2*-mCherry reporters to an ST2-deficient background
243 (Figures 4C-4E). Specifically, *ccl2* foci in ST2$^{-/-}$ mice were much reduced in size compared with
244 wildtype infected mice (Figures 4D and 4E). We then assessed which cells were producing *ccl2*.
245 *ccl2* in infected brain tissue colocalized with both GFAP+ astrocytes and Iba1+ macrophages
246 (Figure 4F). Approximately 75% of cells expressing *ccl2* were astrocytes, 22% were Iba1+
247 macrophages, and 3% of cells did not co-stain with either of these markers (Figure 4G). These
248 results were validated by assessing *ccl2* expression in brain cells magnetically enriched for either
249 astrocytes or macrophages. To enrich for astrocytes, we used a previously validated protocol,
250 which first removes CD11b+ cells by negative magnetic isolation, followed by positive isolation of
251 ACSA-2 positive cells[61]. At the same time, we enriched for CD11b+ myeloid cells by keeping the
252 CD11b+ magnetically-enriched fraction (Figure S5). RNA from these populations showed a 10-
253 fold higher *ccl2* expression in astrocytes compared with macrophages during chronic infection
254 (Figure 4H). Although multiple signals undoubtedly converge to induce chemokine expression
255 such as *ccl2* during infection, including other innate cytokines[62], our data suggest that IL-33 is a
256 major contributor to the induction of local *ccl2*. These results support a role for IL-33 in inducing
257 chemokine production to promote immune cell entry to the brain.

258

259 **IL-33 signals on a radio-resistant cell type to control chronic *T. gondii* infection**

260 In order to further understand how IL-33 signaling supports protective immune responses,
261 we began to narrow down the cell type that directly responds to IL-33 in the brain. In studies
262 concerning IL-33 during CNS disease, genetic evidence for a responding cell type is lacking. This
263 is likely due in part to the fact that several brain-resident cells can express ST2 during disease,
264 such as microglia, astrocytes, and endothelial cells[36,63-65], but a wide range of immune cells can
265 also express the receptor, including but not limited to ILC2s, regulatory T cells, Th2 cells, mast
266 cells, and macrophages[47,66,67]. We performed a bone marrow chimera to determine if IL-33 signals
267 on a radio-sensitive or a radio-resistant cell type to exert its effects during chronic *T. gondii*
268 infection. We lethally irradiated wildtype and ST2$^{-/-}$ mice and reconstituted these mice with bone
269 marrow from either wildtype donors or ST2$^{-/-}$ donors (Figure 5A). Blood was assessed for
270 reconstitution prior to infection (Figures 5B-D), and in all cases, immune cells were >90% positive
271 for the congenic CD45 marker of donor mice, confirming successful reconstitution of the chimera
272 (Figures 5B-D). We note that irradiation did alter the severity of infection, resulting in high parasite
273 burdens in all groups, and a high number of infiltrating cells (Figures 5E-G). Nonetheless, these
274 experiments revealed that ST2-deficiency on radio-resistant cells, recapitulated the phenotype of
275 global knockouts, including reduced infiltrating myeloid and T cell numbers and parasite burden
276 (Figures 5E-G).

277 Importantly, microglia are not fully replenished by bone marrow-derived cells post-
278 irradiation. Therefore, we cannot rule out microglia as responding to IL-33 in the brain. In addition,
279 microglia highly express ST2 at baseline[36,44,45,63], prior to chronic infection. To better understand
280 which radio-resistant cells were capable of responding to IL-33, we magnetically enriched for
281 CD11b+ cells (microglia/macrophages), and ACSA-2+ astrocytes from naïve and chronically
282 infected brain tissue, and compared *il1rl1* (st2) expression. These cell types have been previously

283 reported to express the IL-33 receptor, are major producers of IL-33-dependent chemokine during
284 *T. gondii* infection, and are generally required for control of *T. gondii* infection. We found that
285 microglia/macrophages cells express *il1rl1* at high levels in uninfected mice, but downregulate the
286 IL-33 receptor 20-fold upon infection, while astrocytes express low levels at baseline and increase
287 receptor expression with infection (Figure S6A), thus indicating a change in capability of cells
288 which are able to respond to IL-33 prior to and following infection.
289
290 **IL-33-ST2 signaling on astrocytes, but not microglia/macrophages, potentiates**
291 **immune responses and limits parasite burden**
292 To determine if IL-33 directly signals on microglia/macrophages or astrocytes, we crossed
293 ST2fl/fl mice[68], to either constitutive CX3CR1cre mice or GFAPcre mice, respectively. We
294 observed that deletion of ST2 from macrophages did not affect any major phenotype observed in
295 $ST2^{-/-}$ knockout mice, including brain myeloid cell number and function, T cell number, or parasite
296 burden (Figure 6A-C). We observed minor defects in CD4+ T cell number in these mice, including
297 CD4+ T cell proliferation (Figure 6B). Direct IL-33-ST2 signaling on astrocytes, however, did
298 impact immune cell numbers in the brain, including infiltrating myeloid cell and T cells. T cell
299 function, including proliferation and IFN-γ production, was also reduced in mice with IL-33R-
300 deficient astrocytes (Figures 6D and 6E). Importantly, aligned with a decrease in T cell-derived
301 IFN-γ, which is critical for control of infection[13], GFAPcre ST2fl/fl mice displayed increased
302 parasite burden (Figure 6F). Additionally, GFAPcre ST2fl/fl mice did not have defects in peripheral
303 immune cell compartments, displaying increased immune cell numbers in the spleen during
304 chronic infection (Figure S6B), to a level comparable with whole-body ST2-deficiency.
305 Collectively, these results show that astrocytes respond to a damage signal, IL-33, to promote a
306 protective immune response to *T. gondii* in the brain.
307

308 **DISCUSSION**

309 We observe that brain resident cells can respond to IL-33, a damage-associated molecular
310 pattern (DAMP), to initiate protective immunity during chronic *T. gondii* infection. This work begins
311 to uncover the mechanisms by which the presence of *T. gondii* can be sensed in brain tissue,
312 which is devoid of peripheral immune cells in the healthy state. Indeed, much of the work on
313 sensing of *T. gondii* has focused on immune cell recognition of *T. gondii* in peripheral tissues,
314 during the acute phase of infection. It has been shown that *T. gondii* profilin protein, a pathogen-
315 associated molecular pattern (PAMP), can be sensed directly by TLR11 and TLR12-expressing
316 dendritic cells in the periphery, which are capable of initiating protective Th1 immunity by
317 producing IL-12[8,21,22]. In humans, however, TLR11 is a pseudogene and TLR12 is not
318 expressed[69]. Thus, more recent studies have focused on innate sensing mechanisms with
319 potential relevance to humans, including NOD-like receptor sensing of *T. gondii*[23,24], as well as
320 alarmin recognition, such as S100A11[25], by macrophages. Since we find IL-33 to be highly
321 expressed in human brain tissue, we hypothesize that our results will be relevant to control of
322 human brain infection. Furthermore, our results shed light on the importance of continual DAMP
323 recognition to contain infection long after adaptive immune responses are first primed in
324 peripheral tissues.

325 We found nuclear IL-33 to be expressed by oligodendrocytes and astrocytes in the mouse
326 *T. gondii*-infected brain, and we were able to detect extracellular IL-33 in the cerebrospinal fluid
327 during chronic infection. Since extracellular IL-33 is negatively regulated in a number of ways to
328 limit inflammation[70-72], this result suggests high levels of IL-33 release during brain *T. gondii*
329 infection. Our results also raise the question of how IL-33 is liberated from astrocytes and
330 oligodendrocytes during disease, whether by cell death or secretion[67]. Mechanisms of glial death
331 during disease have not been extensively studied *in vivo*, and it is unclear if the parasite itself, or
332 if secondary, toxic inflammation can mediate the release of host damage signals. It is also unclear
333 how long-ranging the effects of alarmin signaling are. Work on IL-33 in cardiac muscle[68], as well

334 as the retina[73], has indicated that IL-33 often signals very locally, acting in either an autocrine or
335 paracrine manner. For example, Müller cells, specialized astrocytes in the retina, have been
336 implicated in the release and sensing of IL-33 in the retina[73]. Our work further corroborates local
337 IL-33 signaling, as IL-33-dependent *ccl2* expression is found adjacent to necrotic lesions
338 containing replicating *T. gondii*. Thus, IL-33 may be released by astrocytes or oligodendrocytes,
339 and signal on the same cell type, including adjacent cells, to induce chemokine expression
340 necessary for the recruitment of anti-parasitic immune cells to the brain.

341 In the lung, gut, and skin, IL-33 has historically been shown to signal almost exclusively
342 on immune cells to orchestrate immunity[47]. However, recent work demonstrates that IL-33 can
343 signal on non-hematopoeitic cells – including cardiomyocytes in the heart[68] and endothelial cells
344 *in vitro*. We found, consistent with a previous report in stroke[36], that IL-33 signals on a radio-
345 resistant responder during brain *T. gondii* infection. Tissue microenvironment and context likely
346 influence whether IL-33 signaling on immune cells is relevant. Peripheral immune cells are not
347 present in healthy brain tissue due to the blood brain barrier, thus necessitating the capability of
348 brain resident cells to respond to damage. Additionally, the environmental milieu specific to CNS
349 *T. gondii* infection promotes a robust Th-1skewed immune response necessary for intracellular
350 parasite killing, characterized by T-cell derived IFN-γ and macrophage-derived iNOS[6,8]. Thus, the
351 IL-33-dependent mechanisms, specifically those activating type 2 immune responses that drive
352 asthma, allergy, and the expulsion of helminth infections[46,66], may not be relevant to brain infection
353 with an intracellular pathogen.

354 When we examined brain-resident cell expression of ST2, we found that microglia express
355 high levels of ST2 in healthy brain tissue, but they downregulate the receptor 20-fold upon
356 infection. A downshift in microglia inflammatory genes has been reported in other disease states,
357 and it is unclear what factors drive this process. However, these results do not rule out the
358 importance of IL-33 signaling on microglia in other settings. Indeed, during development, microglia
359 expression of ST2 is required for microglial phagocytosis of synapses[44]. While we did not find any

360 major impact of microglia/macrophage ST2 expression on control of chronic *T. gondii* infection, it
361 is possible that microglia respond to IL-33 at earlier timepoints, such as when the parasite first
362 reaches the brain. If microglia normally respond to IL-33 earlier in infection, our results indicate
363 that astrocyte responses to IL-33, or additional MyD88-dependent signals, may compensate for
364 the lack of ST2-signaling in microglia.

365 In contrast to microglia/macrophages, we found that astrocytes increase expression of the
366 IL-33 receptor upon infection. Astrocytes are critical for controlling CNS infection and potentiate
367 inflammation. For example, astrocyte responses to IFN-γ are necessary to control *T. gondii*
368 infection[74]. We found that IL-33 receptor expression on astrocytes was required for adequate
369 promotion of an anti-parasitic immune response in the brain, including proliferation and IFN-γ
370 production in T cells, which is critical for control of *T. gondii*. This is the first time, to our knowledge,
371 that astrocytes have been directly implicated in an IL-33 response via genetic manipulation. Our
372 results also raise questions regarding the role of astrocytes in supporting T cell responses to
373 infection and whether these responses are direct or indirect. IL-33 signals through the adaptor
374 MyD88[66], and could influence the expression of numerous molecules that support T cell
375 responses, including trophic factors, TCR engagement, chemokines, or blood brain barrier
376 opening for T cell entry.

377 Notably, immune defects in GFAPcre ST2fl/fl mice did not match the magnitude observed
378 in $ST2^{-/-}$ mice. These results either implicate compensation by other cell types when ST2 is
379 deleted from a single population, or the presence of additional ST2-expressing radio-resistant cell
380 types not considered here. One possibility is endothelial cells, which have recently been shown
381 to express ST2 during disease and can be directly activated in response to IL-33 *in vitro*[65,75].
382 Nonetheless, our results indicate that astrocytes are capable of responding to extracellular IL-33
383 during infection. This finding, in addition to the detection of IL-33 release in the brain, has broad

384 implications for sensing of tissue damage in other disease states, as definitive evidence that
385 alarmins can signal strictly within brain tissue to initiate protective immunity.

386 Our results underscore the importance of the signaling of one alarmin in controlling chronic
387 *T. gondii* infection. Little is known about the direct recognition of *T. gondii* in brain tissue and we
388 implicate the response to infection-induced damage as a major mechanism of innate immune
389 activation in the brain throughout chronic infection. Numerous canonical alarmins are expressed
390 in the brain and their receptors are differentially expressed by cell type. Thus, there is likely a
391 complex integration of multiple PAMP and DAMP signals that is required to allow peripheral
392 immune cells to overcome the blood brain barrier, infiltrate the tissue parenchyma, and carry out
393 effector function. Identifying the cell types that can repond to specific DAMPs in the brain will be
394 key not only to understanding immunity to CNS infection but any neuroinflammatory condition
395 with hallmarks of cell death, including neurodegeneration.

396

397 **METHODS**

398

399 **Contact for reagent and resource sharing**

400 Further information and requests for resources and reagents should be directed to and will be
401 fulfilled by the Lead Contact, Tajie Harris (tajieharris@virginia.edu).

402

403 **Experimental mice**

404 C57BL/6, CCL2-RFP^{flox}, CCR2^{RFP}, GFAPcre, and CX3CR1cre mice were purchased from
405 Jackson Laboratories. B6.SJL-Ptprc^{a} Pepc^{b}/BoyCrCl (C57BL/6 Ly5.1) mice were purchased from
406 Charles River. Ordering information for these strains is listed in the key resources table.
407 ST2(il1rl1)$^{-/-}$ mice were generously provided by Andrew McKenzie (Cambridge University). IL-33^{-}
408 $^{/-}$ animals were obtained from Amgen by Elia Tait Wojno, currently at the University of Washington
409 and previously at Cornell University. All IL-33-/- animals were housed at Cornell University.

410 ST2(il1rl1)-floxed embryos were received from KOMP repository (RRID MMRRC:048182-UCD).
411 Importantly, we received notice after fully breeding these mice to cre-expressing mice, that the
412 deposited floxed embryos contain a copy of an inducible, cardiomyocyte-driven cre[68], unknown
413 to the KOMP repository. Upon receiving notice, we did detect the presence of MYH6cre^{ERT2} alleles
414 throughout our ST2fl/fl colony. Importantly, we deleted ST2 under the control of constitutive cre
415 drivers and never administered tamoxifen to these mice. We performed statistical tests to
416 determine the effect of MYH6cre expression, and did not find evidence of an effect in experiments
417 where the MYH6cre was present in some animals and not others. Moreover, in the experiments
418 reported here (Figure 6), all animals were positive for the MYH6cre allele. All animals were housed
419 in a UVA specific pathogen-free facility with a 12h light/dark cycle. Mice were age and sex
420 matched for each experiment, and were sacrificed in parallel. Animals were infected with *T. gondii*
421 at 7 to 9 weeks of age and were housed separately from breeding animals. All procedures
422 adhered to regulations of the Institutional Animal Care and Use Committee (ACUC) at the
423 University of Virginia and Cornell University.
424
425 **Human brain tissue**
426 Healthy human brain samples from adult patients were obtained from the UVA Human
427 Biorepository and Tissue Research Facility. Samples were preserved on paraffin embedded
428 slides. Patient identification and medical background was withheld and therefore IRB approval
429 was not required.
430
431 **Parasite strains**
432 The avirulent, type II *Toxoplasma gondii* strain Me49 was used for all infections. *T. gondii* cysts
433 were maintained in chronically infected (1-6 months) Swiss Webster (Charles River) mice. To
434 generate cysts for experimental infections, CBA/J (Jackson Laboratories) mice were infected with
435 10 cysts from brain homogenate of Swiss Webster mice by i.p. injection in 200µl PBS. 5-30 cysts

436 from 4 week-infected CBA/J brain homogenate were then used to infect animals in all
437 experiments.
438
439 **Immunohistochemistry**
440 Mouse Tissue Immunofluorescence:
441 Reporter mice were perfused with 30 mL PBS followed by 30 mL 4% PFA (Electron Microscopy
442 Sciences). All non-reporter strains were only perfused with PBS. Brains were cut along the midline
443 and post-fixed in 4% PFA for 24h at 4°C. Brains were then cryoprotected in 30% sucrose (Sigma)
444 for 24h at 4°C, embedded in OCT (Tissue Tek), and frozen on dry ice. Samples were then stored
445 at -20°C. 40 µm sections were cut using a CM 1950 cryostat (Leica) and placed into a 24-well
446 plate containing PBS. Sections were blocked in PBS containing 2% goat or donkey serum
447 (Jackson ImmunoResearch), 0.1% triton, 0.05% Tween 20, and 1% BSA for 1h at RT. Sections
448 were then incubated with primary antibody diluted in blocking buffer at 4°C overnight. Sections
449 were washed the following day and incubated with secondary antibody in blocking buffer at room
450 temperature for 1h. Sections were then washed and incubated with DAPI (Thermo Scientific) for
451 5 min at RT. Sections were then mounted onto Superfrost microscope slides (Fisherbrand) with
452 aquamount (Lerner Laboratories) and coverslipped (Fisherbrand). Slides were stored at 4°C
453 before use. Images were captured using an TCS SP8 confocal microscope (Leica) and analyzed
454 using Imaris (Bitplane) software. Volumetric analysis was achieved using the surfaces feature of
455 Imaris.
456
457 **Human tissue immunofluorescence:**
458 Slides containing 4 µm sections of human brain tissue were received from the UVA Biorepository
459 and Tissue Research Facility and de-paraffinized in a gradient from 100% xylene (Fisher) to 50%
460 ethanol (Decon Laboratories). Slides were then washed in running water and distilled water.

461 Antigen retrieval was performed by incubating slides in antigen retrieval buffer (10 mM sodium
462 citrate, 0.05%Tween-20, pH 6.0) in an Aroma digital rice cooker for 45 min at 95°C. Slides were
463 then washed in running water followed by PBS-TW. Slides were then incubated with primary and
464 secondary antibodies as described above for mouse brain tissue. Prior to imaging,
465 Autoflourescence Eliminator Reagent was applied per the manufacturer's instructions (EMD
466 Millipore).
467
468 **Tissue processing and flow cytometry**
469 Whole PBS-perfused brains were collected into 4 mL of complete RPMI (cRPMI)(10% fetal bovine
470 serum, 1%NEAA, 1%Pen/Strep, 1%Sodium Pyruvate, 0.1%-β-mercaptoethanol). Papain
471 digestion was performed for the chimera experiment. To perform papain digestion, brains were
472 cut into 6 pieces and incubated in 5 mL HBSS containing 50U/mL DNase (Roche), and 4U/mL
473 papain (Worthington-Biochem) for 45 min at 37°C. Tissue was triturated first with a large bore
474 glass pipette tip, and twice with a small-bore pipette tip every 15 min. In all other experiments
475 collagenase/dispase was used to digest brain tissue. To perform collagenase/dispase digestion,
476 perfused brains were minced using a razor blade and passed through an 18-gauge needle. Brains
477 were then digested with 0.227mg/mL collagenase/dispase and 50U/mL DNase(Roche) for 1h at
478 37°C. Following digestion, homogenate was strained through a 70 µm nylon filter (Corning).
479 Samples were then pelleted and spun in 20 mL 40% Percoll at 650 g for 25 min. Myelin was
480 aspirated and cell pellets were washed with cRPMI. Finally, samples were resuspended in cRPMI
481 and cells were enumerated. Spleens were collected into 4 mL cRPMI and macerated through a
482 40 µM nylon filter (Corning). Samples were pelleted and resuspended in 2 mL RBC lysis buffer
483 (0.16 M NH_4Cl) Samples were then washed with cRPMI, and resuspended for counting and
484 staining. In cases of acute infection, 4mL of peritoneal lavage fluid was pelleted and resuspended
485 in 2mL of cRPMI for counting and staining. Single cell suspensions were pipetted into a 96 well

486 plate and pelleted. Samples were resuspended in 50 μL Fc Block (0.1 μg/ml 2.4G2 Ab (BioXCell),
487 0.1% rat gamma globulin (Jackson Immunoresearch)) for 10 min. Cells were then surface stained
488 in 50 μL FACS buffer (PBS, 0.2% BSA, and 2 mM EDTA) for 30 min at 4°C. Following surface
489 staining, cells were fixed for at least 30 min at 4°C with a fixation/permeabilization kit
490 (eBioscience) and permeabilized (eBioscience). Samples were then incubated with intracellular
491 antibodies in permeabilization buffer for 30 min at 4°C. Samples were run on a Gallios flow
492 cytometer (Beckman Coulter), and analyzed using Flowjo software, v. 10.
493
494 **qRT-PCR**
495 Perfused brain tissue (100 mg) was placed into bead beating tubes (Sarstedt) containing 1mL
496 Trizol reagent (Ambion) and zirconia/silica beads (Biospec). Tissue was homogenized for 30
497 seconds with a Mini-bead beater (Biospec) machine. RNA was extracted following
498 homogenization per the Trizol Reagent manufacturer's instructions. Complementary DNA was
499 then synthesized using a High Capacity Reverse Transcription Kit (Applied Biosystems). Taqman
500 gene expression assays were acquired from Applied Biosystems and are listed in the key
501 resources table. A 2X Taq-based mastermix (Bioline) was used for all reactions and run on a
502 CFX384 Real-Time System (Bio-Rad). Hprt was used as the brain housekeeping gene and
503 relative expression to wildtype controls was calculated as $2^{(-\Delta\Delta CT)}$.
504
505 ***T. gondii* cyst counts**
506 Brain tissue (100 mg) was minced with a razor in 2mL cRPMI. Brain tissue was then passed
507 through an 18 gauge and 22-gauge needle. 30 uL of resulting homogenate was pipetted onto a
508 microscope slide (VWR) and counted on a Brightfield DM 2000 LED microscope (Leica). Cyst
509 counts were extrapolated for whole brains.
510
511 **Bone marrow chimera**

512 Wildtype B6.SJL-Ptprc^{a} Pepc^{b}/BoyJ (C57BL/6 CD45.1) and ST2KO C57BL/6 mice were irradiated
513 with 1000 rad. Irradiated mice received 3x10^{6} bone marrow cells from CD45.1 and CD45.2
514 donors the same day. Bone marrow was transferred by retro-orbital i.v. injection under isoflurane
515 anesthetization. All mice received sulfa-antibiotic water for 2 weeks post-irradiation and were
516 given 6 weeks for bone marrow to reconstitute. At 6 weeks, tail blood was collected from
517 representative mice and assessed for reconstitution by flow cytometry. Mice were then infected
518 for 4 weeks prior to analysis.
519
520 **Brain homogenate *ex vivo* supernatant collection**
521 Brains were harvested from naïve and infected mice. Brain tissue was processed down to a single
522 cell suspension as outlined in "tissue processing and flow cytometry". Cells from half a brain were
523 incubated in a 96-well plate in 200μL for 4 hours at 37°C. Cells were then pelleted at 1500rpm for
524 5 minutes, and supernatant was stored at -80°C for measurement of IL-33 by ELISA.
525
526 **CSF collection**
527 Naïve and infected mice were anesthetized with ketamine/xylazine, their necks were shaved and
528 obstructing skin and tissue surrounding the dura of the cisterna magna was removed. A small
529 glass capillary was inserted into the dura of the cisterna magna, allowing approximately 10μL of
530 CSF to fill the capillary. CSF from 4-5 mice was pooled and frozen at -80°C.
531
532 **IL-33 ELISA**
533 The IL-33 Quantikine ELISA kit was purchased from Applied Biosystems and manufacturer
534 instructions were followed. 50μL of either brain homogenate supernatant (*ex-vivo* assay) or CSF
535 was used as sample volume. 4-5 CSF samples from individual animals were pooled to reach

536 50μL sample volume. IL-33 standards were serially diluted to a minimum of 30pg/mL. Final values
537 of standards and samples were read on a spectrophotometer at 450nm.
538
539 **ACSA-2/CD11b magnetic enrichment**
540 Brain tissue was harvested from mice and processed down to a single cell suspension as
541 described in "tissue processing and flow cytometry" methods. The Anti-ACSA2 and CD11b
542 Microbead kits, purchased from Miltenyi, were used to enrich for astrocytes and macrophages,
543 respectively, over magnetic columns. In the case of enriching for astrocytes, both kits were used
544 to first remove CD11b+ cells and then enrich for ACSA-2+ cells. Double-purifications were
545 performed in all cases, which was optional, but recommended, by Miltenyi's protocol. Cells were
546 pelleted at 1500rpm and stored in 300μL Trizol (Ambion) at -80°C until further use.
547
548 **Statistical analyses**
549 Statistical analyses comparing two groups at one time point were done using a student's t-test in
550 Prism software, v. 7.0a. Statistical analyses comparing more than two groups within the same
551 timepoint or infection were done using a one-way Anova. In instances where data from multiple
552 infections were combined, all from the same time-point post infection, a randomized block ANOVA
553 was performed using R v. 3.4.4 statistical software to account for variability between infections.
554 Genotype was modeled as a fixed effect and experimental day as a random effect. P values are
555 indicated as follows: ns=not significant $p>.05$, * $p < .05$, ** $p < .01$, *** $p < .001$. The number of
556 mice per group, test used, and p values are denoted in each figure legend. Data was graphed
557 using Prism software, v.7.0a.
558

559 # REFERENCES

560

561 1 Wilson, E. H., Weninger, W. & Hunter, C. A. Trafficking of immune cells in the central
562 nervous system. *J Clin Invest* **120**, 1368-1379, doi:10.1172/JCI41911 (2010).
563 2 Hunter, C. A. & Sibley, L. D. Modulation of innate immunity by Toxoplasma gondii
564 virulence effectors. *Nat Rev Microbiol* **10**, 766-778, doi:10.1038/nrmicro2858 (2012).
565 3 Flegr, J., Prandota, J., Sovickova, M. & Israili, Z. H. Toxoplasmosis--a global threat.
566 Correlation of latent toxoplasmosis with specific disease burden in a set of 88 countries.
567 *PLoS One* **9**, e90203, doi:10.1371/journal.pone.0090203 (2014).
568 4 Pappas, G., Roussos, N. & Falagas, M. E. Toxoplasmosis snapshots: global status of
569 Toxoplasma gondii seroprevalence and implications for pregnancy and congenital
570 toxoplasmosis. *Int J Parasitol* **39**, 1385-1394, doi:10.1016/j.ijpara.2009.04.003 (2009).
571 5 Hill, D. & Dubey, J. P. Toxoplasma gondii: transmission, diagnosis and prevention. *Clin*
572 *Microbiol Infect* **8**, 634-640, doi:10.1046/j.1469-0691.2002.00485.x (2002).
573 6 Dupont, C. D., Christian, D. A. & Hunter, C. A. Immune response and immunopathology
574 during toxoplasmosis. *Semin Immunopathol* **34**, 793-813, doi:10.1007/s00281-012-0339-
575 3 (2012).
576 7 Dubey, J. P., Lindsay, D. S. & Speer, C. A. Structures of Toxoplasma gondii tachyzoites,
577 bradyzoites, and sporozoites and biology and development of tissue cysts. *Clin Microbiol*
578 *Rev* **11**, 267-299 (1998).
579 8 Yarovinsky, F. Innate immunity to Toxoplasma gondii infection. *Nat Rev Immunol* **14**,
580 109-121, doi:10.1038/nri3598 (2014).
581 9 Slavin, M. A., Meyers, J. D., Remington, J. S. & Hackman, R. C. Toxoplasma gondii
582 infection in marrow transplant recipients: a 20 year experience. *Bone Marrow Transplant*
583 **13**, 549-557 (1994).
584 10 Luft, B. J. & Remington, J. S. Toxoplasmic encephalitis in AIDS. *Clin Infect Dis* **15**, 211-
585 222 (1992).
586 11 Luft, B. J. & Remington, J. S. AIDS commentary. Toxoplasmic encephalitis. *J Infect Dis*
587 **157**, 1-6 (1988).
588 12 Hunter, C. A. & Remington, J. S. Immunopathogenesis of toxoplasmic encephalitis. *J*
589 *Infect Dis* **170**, 1057-1067 (1994).
590 13 Gazzinelli, R., Xu, Y., Hieny, S., Cheever, A. & Sher, A. Simultaneous depletion of CD4+
591 and CD8+ T lymphocytes is required to reactivate chronic infection with Toxoplasma
592 gondii. *J Immunol* **149**, 175-180 (1992).
593 14 Fox, B. A., Gigley, J. P. & Bzik, D. J. Toxoplasma gondii lacks the enzymes required for
594 de novo arginine biosynthesis and arginine starvation triggers cyst formation. *Int J*
595 *Parasitol* **34**, 323-331, doi:10.1016/j.ijpara.2003.12.001 (2004).
596 15 Scharton-Kersten, T. M., Yap, G., Magram, J. & Sher, A. Inducible nitric oxide is
597 essential for host control of persistent but not acute infection with the intracellular
598 pathogen Toxoplasma gondii. *J Exp Med* **185**, 1261-1273 (1997).
599 16 Yap, G. S. & Sher, A. Effector cells of both nonhemopoietic and hemopoietic origin are
600 required for interferon (IFN)-gamma- and tumor necrosis factor (TNF)-alpha-dependent
601 host resistance to the intracellular pathogen, Toxoplasma gondii. *J Exp Med* **189**, 1083-
602 1092 (1999).
603 17 Chao, C. C., Hu, S., Molitor, T. W., Shaskan, E. G. & Peterson, P. K. Activated microglia
604 mediate neuronal cell injury via a nitric oxide mechanism. *J Immunol* **149**, 2736-2741
605 (1992).

606 18 Yamamoto, M. *et al.* A cluster of interferon-gamma-inducible p65 GTPases plays a
607 critical role in host defense against Toxoplasma gondii. *Immunity* **37**, 302-313,
608 doi:10.1016/j.immuni.2012.06.009 (2012).
609 19 Degrandi, D. *et al.* Extensive characterization of IFN-induced GTPases mGBP1 to
610 mGBP10 involved in host defense. *J Immunol* **179**, 7729-7740 (2007).
611 20 Kresse, A. *et al.* Analyses of murine GBP homology clusters based on in silico, in vitro
612 and in vivo studies. *BMC Genomics* **9**, 158, doi:10.1186/1471-2164-9-158 (2008).
613 21 Yarovinsky, F. *et al.* TLR11 activation of dendritic cells by a protozoan profilin-like
614 protein. *Science* **308**, 1626-1629, doi:10.1126/science.1109893 (2005).
615 22 Koblansky, A. A. *et al.* Recognition of profilin by Toll-like receptor 12 is critical for host
616 resistance to Toxoplasma gondii. *Immunity* **38**, 119-130,
617 doi:10.1016/j.immuni.2012.09.016 (2013).
618 23 Gorfu, G. *et al.* Dual role for inflammasome sensors NLRP1 and NLRP3 in murine
619 resistance to Toxoplasma gondii. *MBio* **5**, doi:10.1128/mBio.01117-13 (2014).
620 24 Ewald, S. E., Chavarria-Smith, J. & Boothroyd, J. C. NLRP1 is an inflammasome sensor
621 for Toxoplasma gondii. *Infect Immun* **82**, 460-468, doi:10.1128/IAI.01170-13 (2014).
622 25 Safronova, A. *et al.* Alarmin S100A11 initiates a chemokine response to the human
623 pathogen Toxoplasma gondii. *Nat Immunol* **20**, 64-72, doi:10.1038/s41590-018-0250-8
624 (2019).
625 26 Worbs, T., Hammerschmidt, S. I. & Forster, R. Dendritic cell migration in health and
626 disease. *Nat Rev Immunol* **17**, 30-48, doi:10.1038/nri.2016.116 (2017).
627 27 Matyszak, M. K. & Perry, V. H. The potential role of dendritic cells in immune-mediated
628 inflammatory diseases in the central nervous system. *Neuroscience* **74**, 599-608 (1996).
629 28 Schaeffer, M. *et al.* Dynamic imaging of T cell-parasite interactions in the brains of mice
630 chronically infected with Toxoplasma gondii. *J Immunol* **182**, 6379-6393,
631 doi:10.4049/jimmunol.0804307 (2009).
632 29 Ferguson, D. J., Graham, D. I. & Hutchison, W. M. Pathological changes in the brains of
633 mice infected with Toxoplasma gondii: a histological, immunocytochemical and
634 ultrastructural study. *Int J Exp Pathol* **72**, 463-474 (1991).
635 30 Drogemuller, K. *et al.* Astrocyte gp130 expression is critical for the control of
636 Toxoplasma encephalitis. *J Immunol* **181**, 2683-2693 (2008).
637 31 Frenkel, J. K. Pathology and pathogenesis of congenital toxoplasmosis. *Bull N Y Acad*
638 *Med* **50**, 182-191 (1974).
639 32 Frenkel, J. K. Pathophysiology of toxoplasmosis. *Parasitol Today* **4**, 273-278 (1988).
640 33 Schmitz, J. *et al.* IL-33, an interleukin-1-like cytokine that signals via the IL-1 receptor-
641 related protein ST2 and induces T helper type 2-associated cytokines. *Immunity* **23**, 479-
642 490, doi:10.1016/j.immuni.2005.09.015 (2005).
643 34 Jones, L. A. *et al.* IL-33 receptor (T1/ST2) signalling is necessary to prevent the
644 development of encephalitis in mice infected with Toxoplasma gondii. *Eur J Immunol* **40**,
645 426-436, doi:10.1002/eji.200939705 (2010).
646 35 Luo, Y. *et al.* Interleukin-33 ameliorates ischemic brain injury in experimental stroke
647 through promoting Th2 response and suppressing Th17 response. *Brain Res* **1597**, 86-
648 94, doi:10.1016/j.brainres.2014.12.005 (2015).
649 36 Yang, Y. *et al.* ST2/IL-33-Dependent Microglial Response Limits Acute Ischemic Brain
650 Injury. *J Neurosci* **37**, 4692-4704, doi:10.1523/JNEUROSCI.3233-16.2017 (2017).
651 37 Fu, A. K. *et al.* IL-33 ameliorates Alzheimer's disease-like pathology and cognitive
652 decline. *Proc Natl Acad Sci U S A* **113**, E2705-2713, doi:10.1073/pnas.1604032113
653 (2016).
654 38 Carlock, C. *et al.* Interleukin33 deficiency causes tau abnormality and
655 neurodegeneration with Alzheimer-like symptoms in aged mice. *Transl Psychiatry* **7**,
656 e1164, doi:10.1038/tp.2017.142 (2017).

657 39 Li, M., Li, Y., Liu, X., Gao, X. & Wang, Y. IL-33 blockade suppresses the development of
658 experimental autoimmune encephalomyelitis in C57BL/6 mice. *J Neuroimmunol* **247**, 25-
659 31, doi:10.1016/j.jneuroim.2012.03.016 (2012).
660 40 Jiang, H. R. *et al.* IL-33 attenuates EAE by suppressing IL-17 and IFN-gamma
661 production and inducing alternatively activated macrophages. *Eur J Immunol* **42**, 1804-
662 1814, doi:10.1002/eji.201141947 (2012).
663 41 Besnard, A. G. *et al.* IL-33-mediated protection against experimental cerebral malaria is
664 linked to induction of type 2 innate lymphoid cells, M2 macrophages and regulatory T
665 cells. *PLoS Pathog* **11**, e1004607, doi:10.1371/journal.ppat.1004607 (2015).
666 42 Reverchon, F. *et al.* IL-33 receptor ST2 regulates the cognitive impairments associated
667 with experimental cerebral malaria. *PLoS Pathog* **13**, e1006322,
668 doi:10.1371/journal.ppat.1006322 (2017).
669 43 Bonilla, W. V. *et al.* The alarmin interleukin-33 drives protective antiviral CD8(+) T cell
670 responses. *Science* **335**, 984-989, doi:10.1126/science.1215418 (2012).
671 44 Vainchtein, I. D. *et al.* Astrocyte-derived interleukin-33 promotes microglial synapse
672 engulfment and neural circuit development. *Science* **359**, 1269-1273,
673 doi:10.1126/science.aal3589 (2018).
674 45 Gadani, S. P., Walsh, J. T., Smirnov, I., Zheng, J. & Kipnis, J. The glia-derived alarmin
675 IL-33 orchestrates the immune response and promotes recovery following CNS injury.
676 *Neuron* **85**, 703-709, doi:10.1016/j.neuron.2015.01.013 (2015).
677 46 Liew, F. Y., Girard, J. P. & Turnquist, H. R. Interleukin-33 in health and disease. *Nat Rev*
678 *Immunol* **16**, 676-689, doi:10.1038/nri.2016.95 (2016).
679 47 Martin, N. T. & Martin, M. U. Interleukin 33 is a guardian of barriers and a local alarmin.
680 *Nat Immunol* **17**, 122-131, doi:10.1038/ni.3370 (2016).
681 48 Saeij, J. P., Boyle, J. P., Grigg, M. E., Arrizabalaga, G. & Boothroyd, J. C.
682 Bioluminescence imaging of Toxoplasma gondii infection in living mice reveals dramatic
683 differences between strains. *Infect Immun* **73**, 695-702, doi:10.1128/IAI.73.2.695-
684 702.2005 (2005).
685 49 Zhang, Y. *et al.* Purification and Characterization of Progenitor and Mature Human
686 Astrocytes Reveals Transcriptional and Functional Differences with Mouse. *Neuron* **89**,
687 37-53, doi:10.1016/j.neuron.2015.11.013 (2016).
688 50 Black, M. W. & Boothroyd, J. C. Lytic cycle of Toxoplasma gondii. *Microbiol Mol Biol Rev*
689 **64**, 607-623 (2000).
690 51 Wen, X. *et al.* Predominant interferon-gamma-mediated expression of CXCL9, CXCL10,
691 and CCL5 proteins in the brain during chronic infection with Toxoplasma gondii in
692 BALB/c mice resistant to development of toxoplasmic encephalitis. *J Interferon Cytokine*
693 *Res* **30**, 653-660, doi:10.1089/jir.2009.0119 (2010).
694 52 Strack, A., Asensio, V. C., Campbell, I. L., Schluter, D. & Deckert, M. Chemokines are
695 differentially expressed by astrocytes, microglia and inflammatory leukocytes in
696 Toxoplasma encephalitis and critically regulated by interferon-gamma. *Acta Neuropathol*
697 **103**, 458-468, doi:10.1007/s00401-001-0491-7 (2002).
698 53 Wang, X., Michie, S. A., Xu, B. & Suzuki, Y. Importance of IFN-gamma-mediated
699 expression of endothelial VCAM-1 on recruitment of CD8+ T cells into the brain during
700 chronic infection with Toxoplasma gondii. *J Interferon Cytokine Res* **27**, 329-338,
701 doi:10.1089/jir.2006.0154 (2007).
702 54 Gazzinelli, R. T., Hieny, S., Wynn, T. A., Wolf, S. & Sher, A. Interleukin 12 is required for
703 the T-lymphocyte-independent induction of interferon gamma by an intracellular parasite
704 and induces resistance in T-cell-deficient hosts. *Proc Natl Acad Sci U S A* **90**, 6115-
705 6119, doi:10.1073/pnas.90.13.6115 (1993).
706 55 Biswas, A. *et al.* Ly6C(high) monocytes control cerebral toxoplasmosis. *J Immunol* **194**,
707 3223-3235, doi:10.4049/jimmunol.1402037 (2015).

708 56 Adams, L. B., Hibbs, J. B., Jr., Taintor, R. R. & Krahenbuhl, J. L. Microbiostatic effect of
709 murine-activated macrophages for Toxoplasma gondii. Role for synthesis of inorganic
710 nitrogen oxides from L-arginine. *J Immunol* **144**, 2725-2729 (1990).
711 57 Harris, T. H. *et al.* Generalized Levy walks and the role of chemokines in migration of
712 effector CD8+ T cells. *Nature* **486**, 545-548, doi:10.1038/nature11098 (2012).
713 58 Kang, Z. *et al.* Act1 mediates IL-17-induced EAE pathogenesis selectively in NG2+ glial
714 cells. *Nat Neurosci* **16**, 1401-1408, doi:10.1038/nn.3505 (2013).
715 59 Ellis, S. L. *et al.* The cell-specific induction of CXC chemokine ligand 9 mediated by IFN-
716 gamma in microglia of the central nervous system is determined by the myeloid
717 transcription factor PU.1. *J Immunol* **185**, 1864-1877, doi:10.4049/jimmunol.1000900
718 (2010).
719 60 Shi, C. *et al.* Bone marrow mesenchymal stem and progenitor cells induce monocyte
720 emigration in response to circulating toll-like receptor ligands. *Immunity* **34**, 590-601,
721 doi:10.1016/j.immuni.2011.02.016 (2011).
722 61 Holt, L. M. & Olsen, M. L. Novel Applications of Magnetic Cell Sorting to Analyze Cell-
723 Type Specific Gene and Protein Expression in the Central Nervous System. *PLoS One*
724 **11**, e0150290, doi:10.1371/journal.pone.0150290 (2016).
725 62 Shi, C. & Pamer, E. G. Monocyte recruitment during infection and inflammation. *Nat Rev*
726 *Immunol* **11**, 762-774, doi:10.1038/nri3070 (2011).
727 63 Yasuoka, S. *et al.* Production and functions of IL-33 in the central nervous system. *Brain*
728 *Res* **1385**, 8-17, doi:10.1016/j.brainres.2011.02.045 (2011).
729 64 Fairlie-Clarke, K. *et al.* Expression and Function of IL-33/ST2 Axis in the Central
730 Nervous System Under Normal and Diseased Conditions. *Front Immunol* **9**, 2596,
731 doi:10.3389/fimmu.2018.02596 (2018).
732 65 Cao, K. *et al.* IL-33/ST2 plays a critical role in endothelial cell activation and microglia-
733 mediated neuroinflammation modulation. *J Neuroinflammation* **15**, 136,
734 doi:10.1186/s12974-018-1169-6 (2018).
735 66 Liew, F. Y., Pitman, N. I. & McInnes, I. B. Disease-associated functions of IL-33: the new
736 kid in the IL-1 family. *Nat Rev Immunol* **10**, 103-110, doi:10.1038/nri2692 (2010).
737 67 Molofsky, A. B., Savage, A. K. & Locksley, R. M. Interleukin-33 in Tissue Homeostasis,
738 Injury, and Inflammation. *Immunity* **42**, 1005-1019, doi:10.1016/j.immuni.2015.06.006
739 (2015).
740 68 Chen, W. Y., Hong, J., Gannon, J., Kakkar, R. & Lee, R. T. Myocardial pressure
741 overload induces systemic inflammation through endothelial cell IL-33. *Proc Natl Acad*
742 *Sci U S A* **112**, 7249-7254, doi:10.1073/pnas.1424236112 (2015).
743 69 Roach, J. C. *et al.* The evolution of vertebrate Toll-like receptors. *Proc Natl Acad Sci U S*
744 *A* **102**, 9577-9582, doi:10.1073/pnas.0502272102 (2005).
745 70 Cayrol, C. & Girard, J. P. The IL-1-like cytokine IL-33 is inactivated after maturation by
746 caspase-1. *Proc Natl Acad Sci U S A* **106**, 9021-9026, doi:10.1073/pnas.0812690106
747 (2009).
748 71 Cohen, E. S. *et al.* Oxidation of the alarmin IL-33 regulates ST2-dependent
749 inflammation. *Nat Commun* **6**, 8327, doi:10.1038/ncomms9327 (2015).
750 72 Bandara, G., Beaven, M. A., Olivera, A., Gilfillan, A. M. & Metcalfe, D. D. Activated mast
751 cells synthesize and release soluble ST2-a decoy receptor for IL-33. *Eur J Immunol* **45**,
752 3034-3044, doi:10.1002/eji.201545501 (2015).
753 73 Xi, H. *et al.* IL-33 amplifies an innate immune response in the degenerating retina. *J Exp*
754 *Med* **213**, 189-207, doi:10.1084/jem.20150894 (2016).
755 74 Hidano, S. *et al.* STAT1 Signaling in Astrocytes Is Essential for Control of Infection in the
756 Central Nervous System. *mBio* **7**, doi:10.1128/mBio.01881-16 (2016).

757 75 Gautier, V. *et al.* Extracellular IL-33 cytokine, but not endogenous nuclear IL-33,
758 regulates protein expression in endothelial cells. *Sci Rep* **6**, 34255,
759 doi:10.1038/srep34255 (2016).
760

761 **FIGURES**

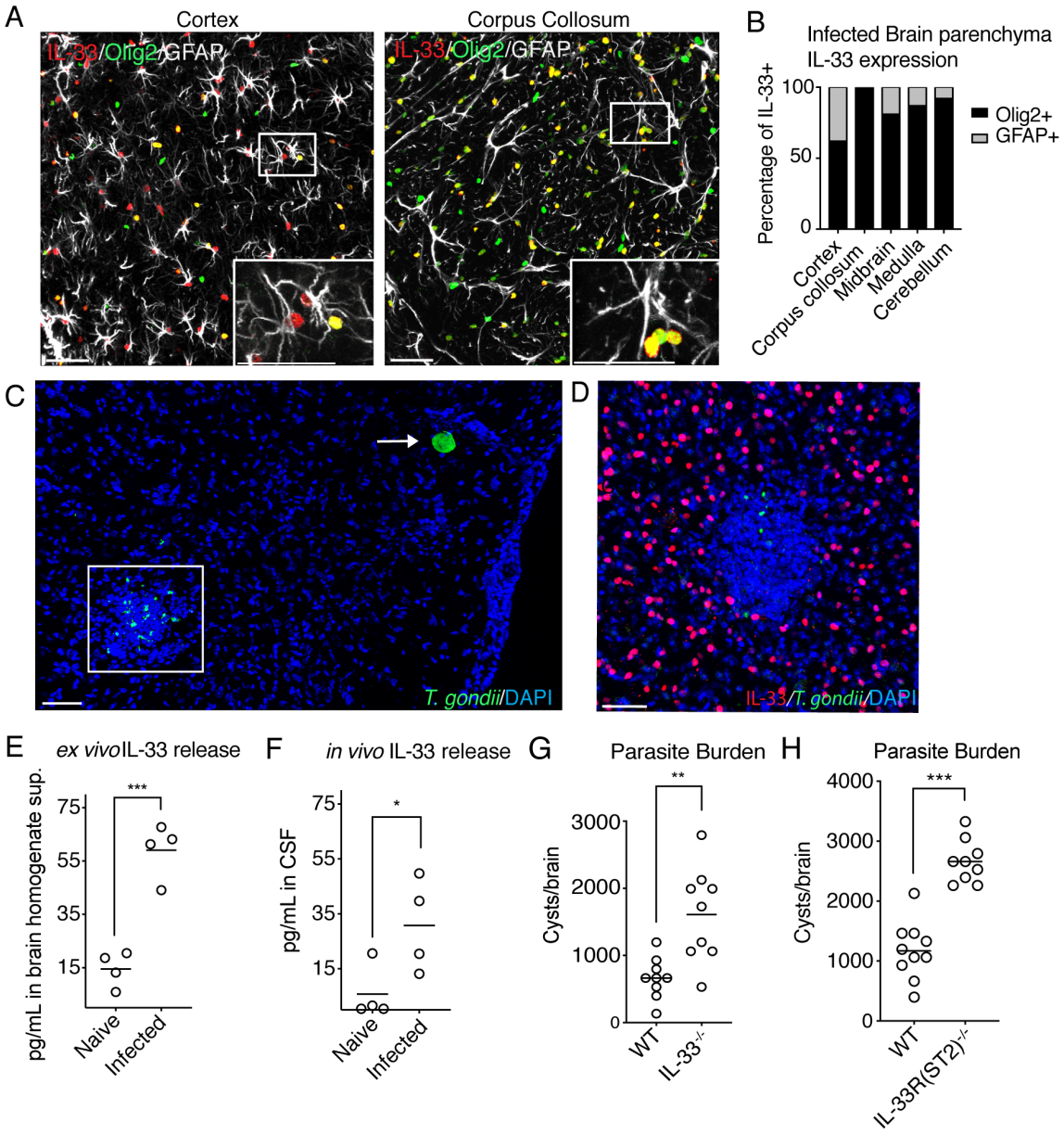

762

763 **Figure 1. IL-33 is expressed by oligodendrocytes and astrocytes during brain *T. gondii* infection, is**

764 **released during infection, and is required for control of parasite. (A and B)** Representatitive images

765 (A) and percentage quantification (B) of nuclear IL-33 expression (red) by cell type four weeks post-infection

766 in various brain regions by confocal fluorescent microscopy. IL-33 is costained with the nuclear

767 oligodendrocyte marker, Olig2 (green) or activated astrocyte marker, GFAP, (white). **(C and D)**

768 Representative images of *T. gondii* in brain tissue, either in cyst form (arrow), or reactivated individual

769 parasites (box)(C). IL-33-positive cells are absent from inflammatory foci containing replicating parasites

770 (D). **(E and F)** Extracellular IL-33 release as measured by ELISA after *ex vivo* incubation of all cells isolated
771 from infected brain tissue (E), or from CSF samples, each dot represents pooled CSF from 4-5 individual
772 mice from a separate infection, displaying four infections in total (F). **(G and H)** Parasite burden as
773 measured by cyst count from brain homogenate of IL-33-deficient (G) and IL-33 receptor (ST2)-deficient
774 mice (H). Statistical significance was determined by two-tailed t-test (E) or randomized block ANOVA, when
775 results from multiple independent experiments are shown (F-H). *= $p<.05$, **= $p<.01$, ***= $p<.001$. Scale
776 bars indicate 50μm.

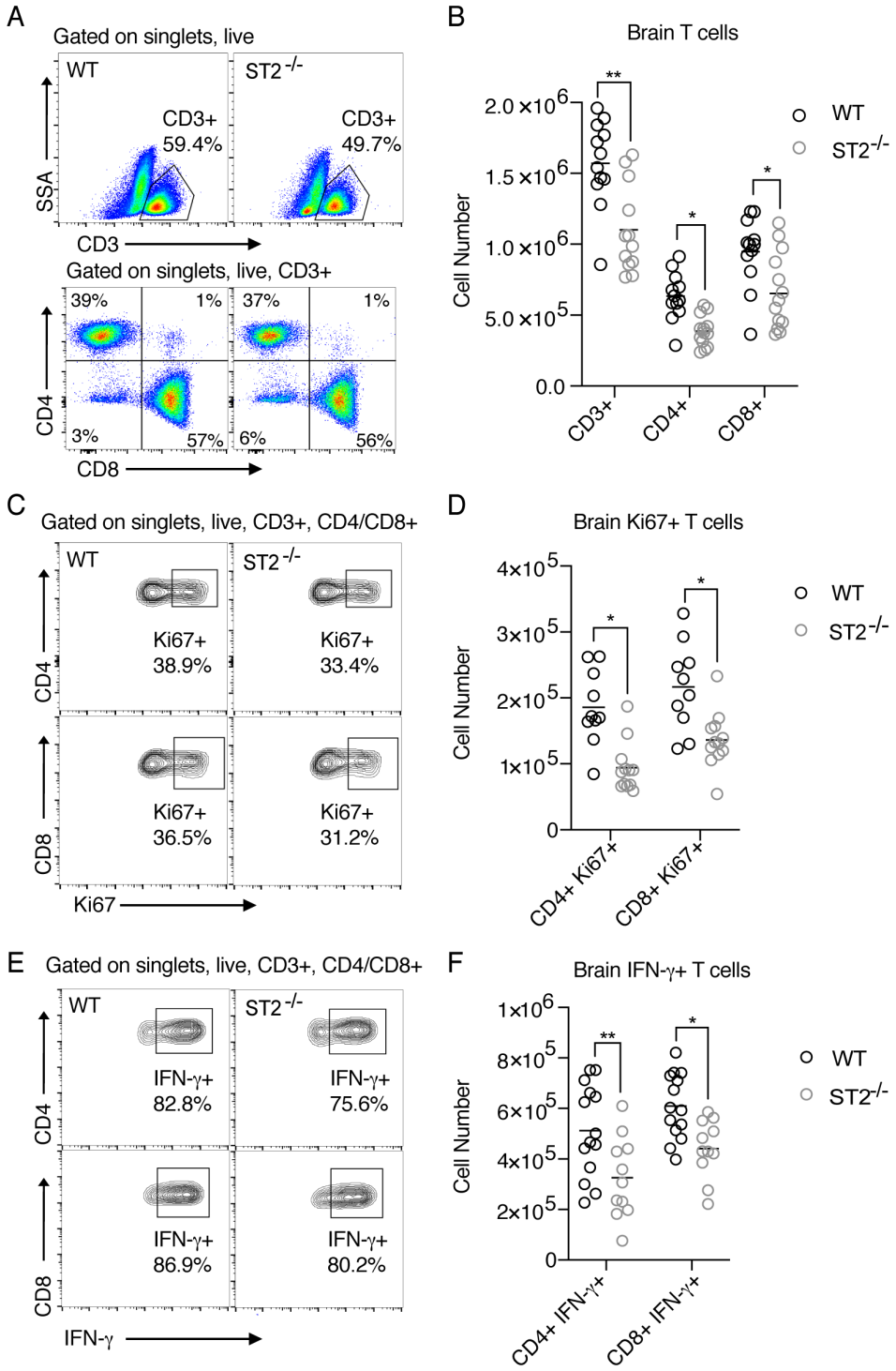

Figure 2. IL-33-ST2 signaling is required for adequate numbers and functionality of T cells in the brain during chronic *T. gondii* infection. (A and B) Representative flow cytometry plots (A) and quantification (B) of infiltrated total T cells in infected brain tissue four weeks-post infection. **(C and D)** Representative flow cytometry plots (C) and quantification (D) showing frequency of proliferating (Ki67+) T

782 subsets in infected brain tissue. **(E and F)** Representative flow cytometry plots (E) and number (F) of IFN-
783 γ-positive T cell subsets in infected brain tissue. IFN-γ was measured following *ex-vivo* re-stimulation of
784 brain cells, incubated with Brefeldin A and PMA/ionomycin for 5 hours at 37°C (F). Statistical significance
785 was determined by randomized block ANOVA (B,D,F), and each quantified panel displays three pooled
786 independent experiments. *= $p<.05$, **= $p<.01$, ***= $p<.001$

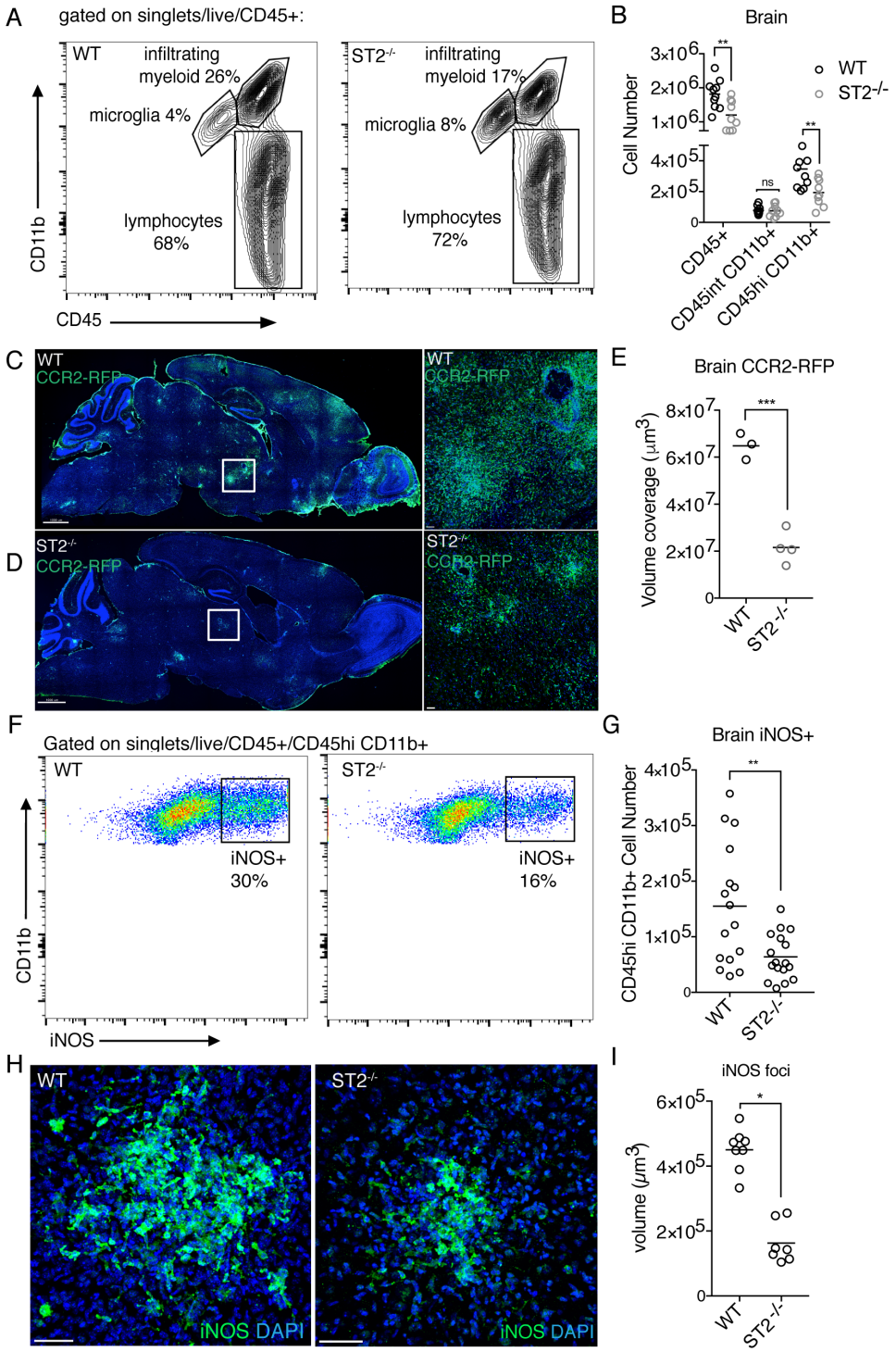

787

788 **Figure 3. IL-33-ST2 signaling is required for the recruitment and anti-parasitic function of peripheral**

789 **myeloid cells in the brain during chronic *T. gondi* infection. (A and B)** Representative flow cytometry

790 plots (A) and quantification (B) of CD11b+ myeloid cells in the brain 4 weeks post infection. CD45hi

791 expression was used to differentiate infiltrating myeloid cells from CD45int microglia. **(C-E)** Visualization (C

792 and D), and quantification (E) of infiltrated CCR2+ monocytes by fluorescence confocal microscopy of
793 **i**nfected CCR2-RFP reporter mice. ST2-deficient mice were crossed to CCR2-RFP mice to assess the
794 contribution of IL-33-ST2 signaling to monocyte recruitment. **(F and G)** Representative flow cytometry plots
795 (F) and quantification (G) of iNOS+ CD45hi, CD11b+ infiltrating cells in the brain. **(H and I)** Visualization
796 (H) and quantification (I) of the size of iNOS foci in brain tissue by fluorescence confocal microscopy.
797 Statistical significance was determined by randomized block ANOVA when two or more experiments were
798 pooled (B, G, I), and by a two-tailed t-test (E). *= $p<.05$, **= $p<.01$, ***= $p<.001$. Scale bars indicate 2000μm
799 (C,D) and 50μm (H).

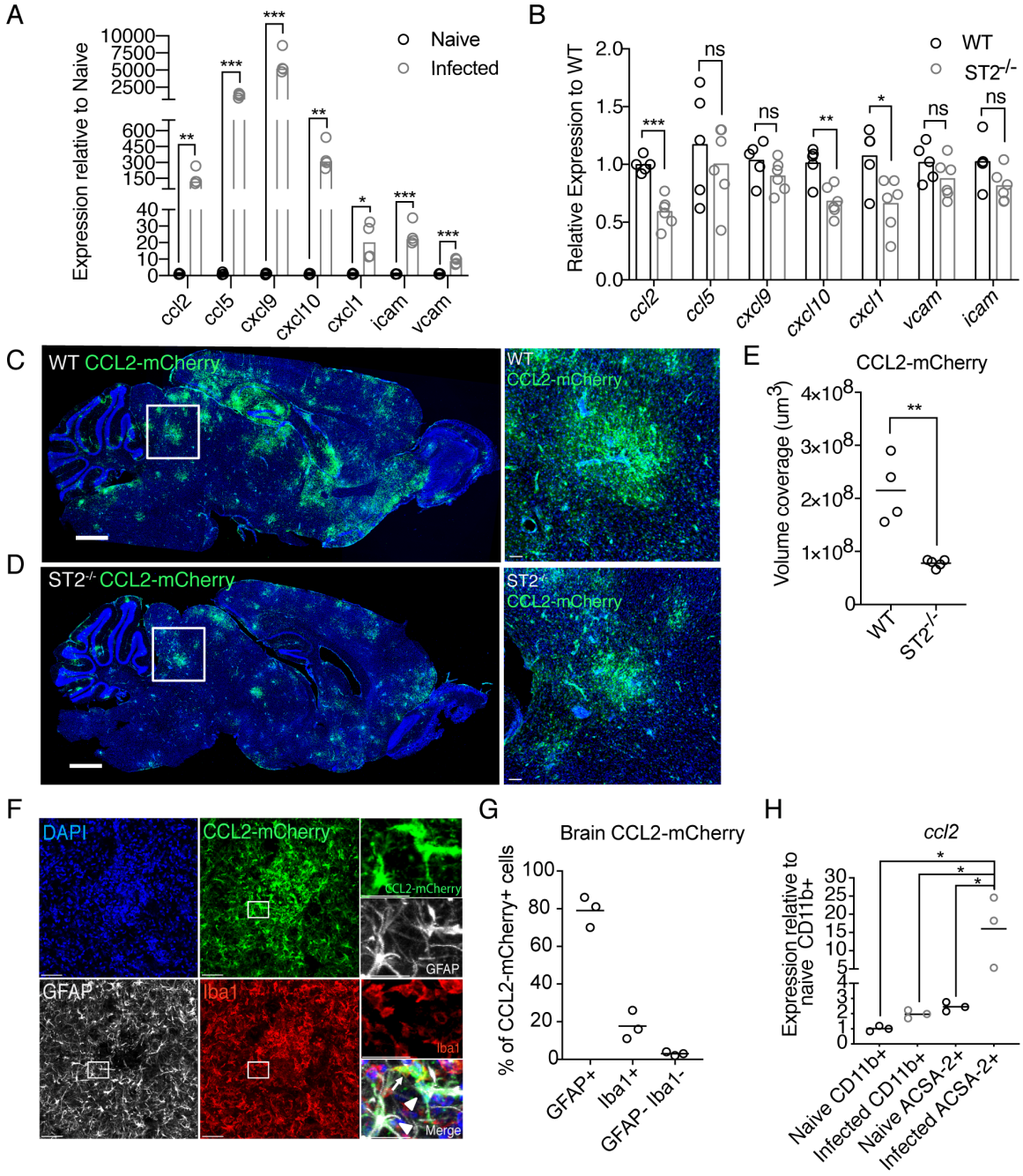

Figure 4. IL-33-ST2 signaling induces factors which recruit immune cells to the brain. (A and B) Real time PCR from whole brain homogenate was used to assess changes in chemokine and adhesion factor gene expression from naïve to infected animals (A) and between wildtype and ST2-deficient animals (B) at four weeks post infection. **(C-E)** Visualization (C,D) and quantification (E) of CCL2-RFP reporter expression by mCherry staining (green) in infected brain tissue by confocal fluorescence microscopy. **(F and G)**

806 Breakdown of CCL2-mCherry reporter positivity by cell type using confocal microscopy. mCherry (green)
807 is colocalized with Iba1+ macrophages (red) or activated, GFAP+ astrocytes (white). **(H)** Cell-type specific
808 magnetic enrichment for myeloid cells (CD11b+) or astrocytes (CD11b- and ACSA-2+) in naïve and
809 chronically infected brain tissue. Single cell suspensions of enriched cells were resuspended in Trizol, RNA
810 extracted, and run by real time PCR for *ccl2* expression. Statistical significance was determined by two-
811 tailed t-test (A, B, E) or One-way ANOVA with Tukey's test (H). *= $p<.05$, **= $p<.01$, ***= $p<.001$. Scale bars
812 indicate 2000μm (C,D) and 50μm (F).

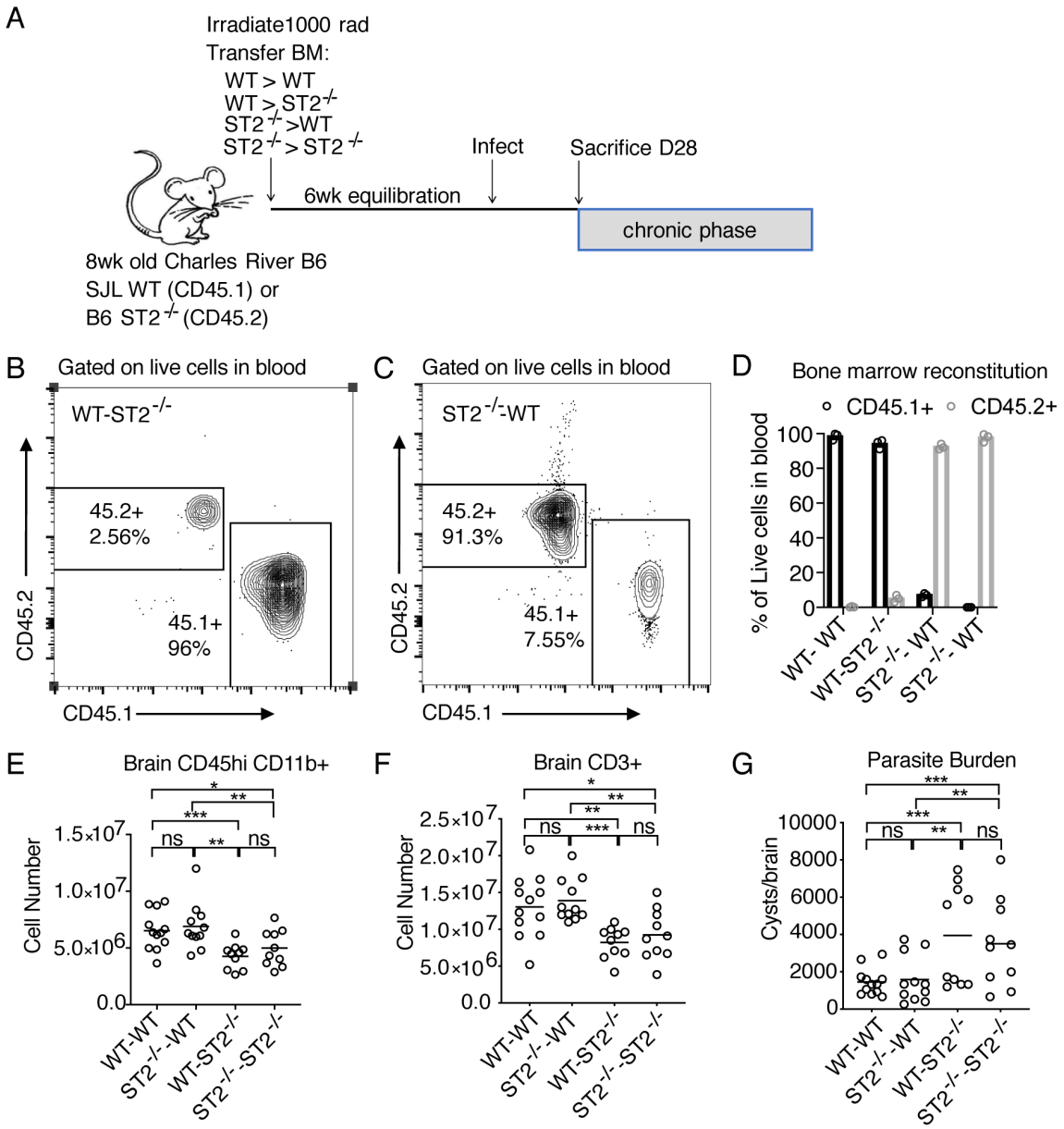

Figure 5. IL-33 signals on a radio-resistant responder. (A) Bone marrow chimera experimental setup. **(B-D)** Representative flow cytometry plots (B,C) and quantification (D) of bone marrow reconstitution in blood 6 weeks post irradiation and prior to infection. **(E and F)** Quantification of immune cells, including infiltrating myeloid cells (E) and T cells (F) in the brain at 4 weeks post infection following irradiation. **(G)** Parasite burden as assessed by cyst count of brain homogenate. Statistical significance was determined by randomized block ANOVA (E-G), each panel showing data pooled from two independent experiments *= p<.05, **= p<.01, ***= p<.001.

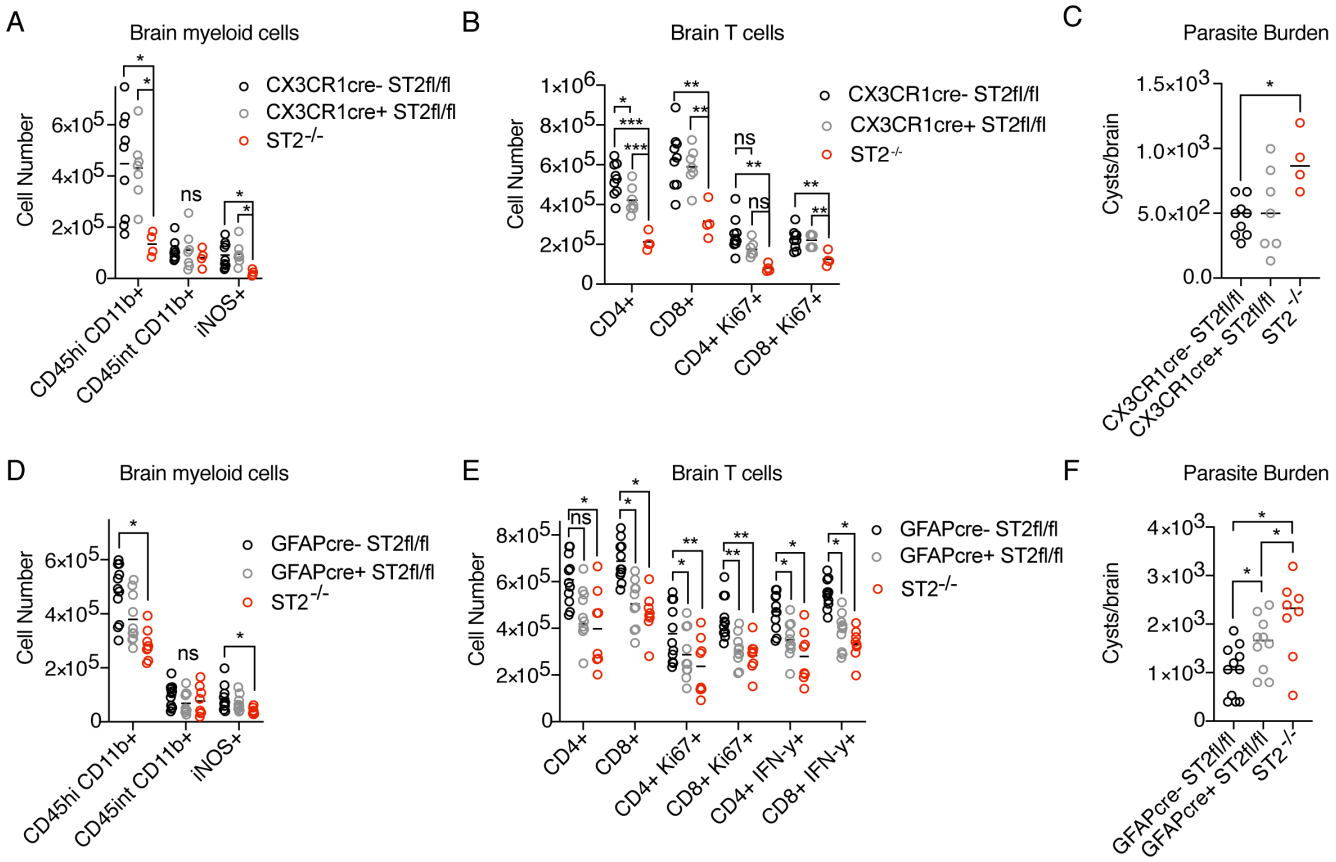

Figure 6. IL-33-ST2 signaling on astrocytes, but not macrophages, is required to control brain *T. gondii* infection (A and B) Quantification of brain immune cells in CX3CR1cre ST2fl/fl mice by flow cytometry – including myeloid cells (A) and T cell subsets (B) at four weeks post infection. **(C)** Parasite burden in CX3CR1cre ST2fl/fl mice as assessed by cyst enumeration in brain homogenate. **(D and E)** Quantification of brain immune cells in GFAPcre ST2fl/fl mice by flow cytometry – including myeloid cells (D) and T cell subsets (E). IFN-γ was measured following *ex-vivo* re-stimulation of brain cells, incubated with Brefeldin A, and PMA/ionomycin for 5 hours at 37°C. **(F)** Parasite burden in GFAPcre ST2fl/fl mice as assessed by cyst enumeration in brain homogenate. Statistical significance was determined by one-way ANOVA with Tukey's test (A-C), or by randomized block ANOVA(D-F), where each panel shows data pooled from two independent experiments *= p<.05, **= p<.01, ***= p<.001.

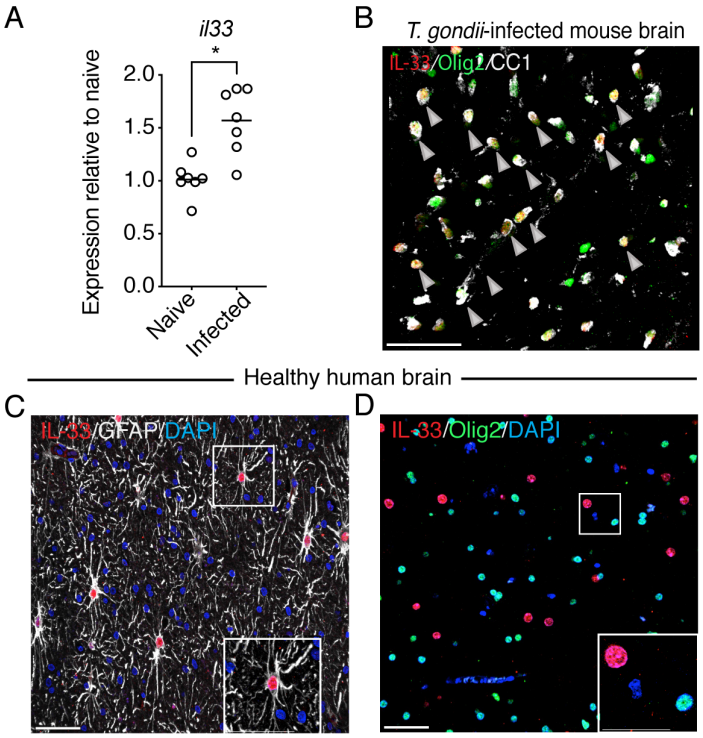

Figure S1. IL-33 expression in mouse and human brain tissue. (A) Real time PCR for IL-33 transcript from whole brain homogente at 4 weeks post infection compared to naïve brain tissue. **(B)** Colocalization, denoted by gray arrows, of nuclear IL-33 (red) with mature oligodendrocytes, marked by nuclear Olig2 expression (green), and CC1(white) by confocal fluorescence microscopy of infected mouse brain tissue. **(C and D)** Confocal fluorescence microscopy of nuclear IL-33 stain present in astrocytes (C) but not oligodendrocytes (D) in the healthy human temporal lobe. Statistical significance was determined by randomized block ANOVA (A), which shows data pooled from two independent experiments *= $p<.05$, **= $p<.01$, ***= $p<.001$. Scale bars indicate 50μm.

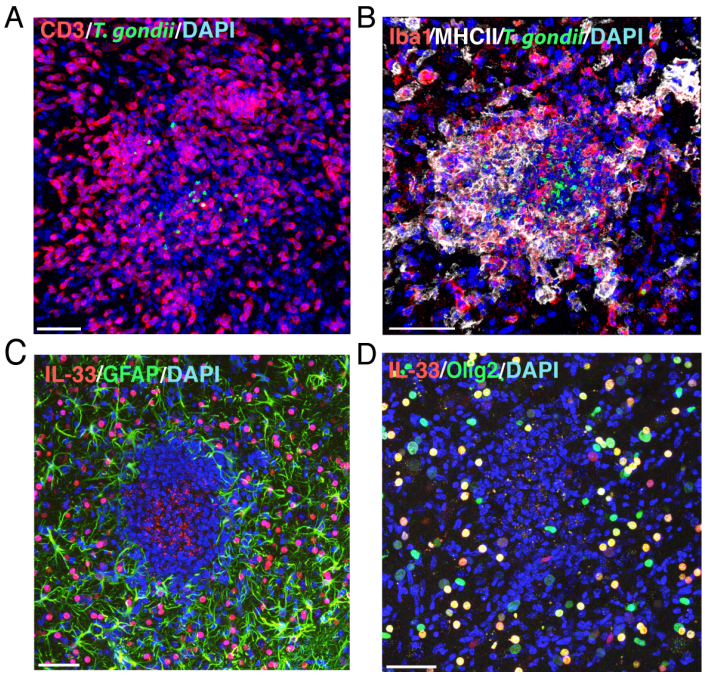

842

843 **Figure S2. Inflammatory lesions in *T.gondii*-infected brain tissue. (A and B)** Representative images of
844 immune cells surrounding foci of individual replicating parasites (green) in cortical brain tissue, including
845 CD3+ T cells (red) (A), and MHCII+ (white) Iba1+ (red) myeloid cells (B). **(C and D)** Representative images
846 of necrotic foci, featuring a loss of brain resident cells which express IL-33 (red), including GFAP+
847 astrocytes (green) (C), and Olig2+ oligodendrocytes (green) (D). Scale bars indicate 50μm.

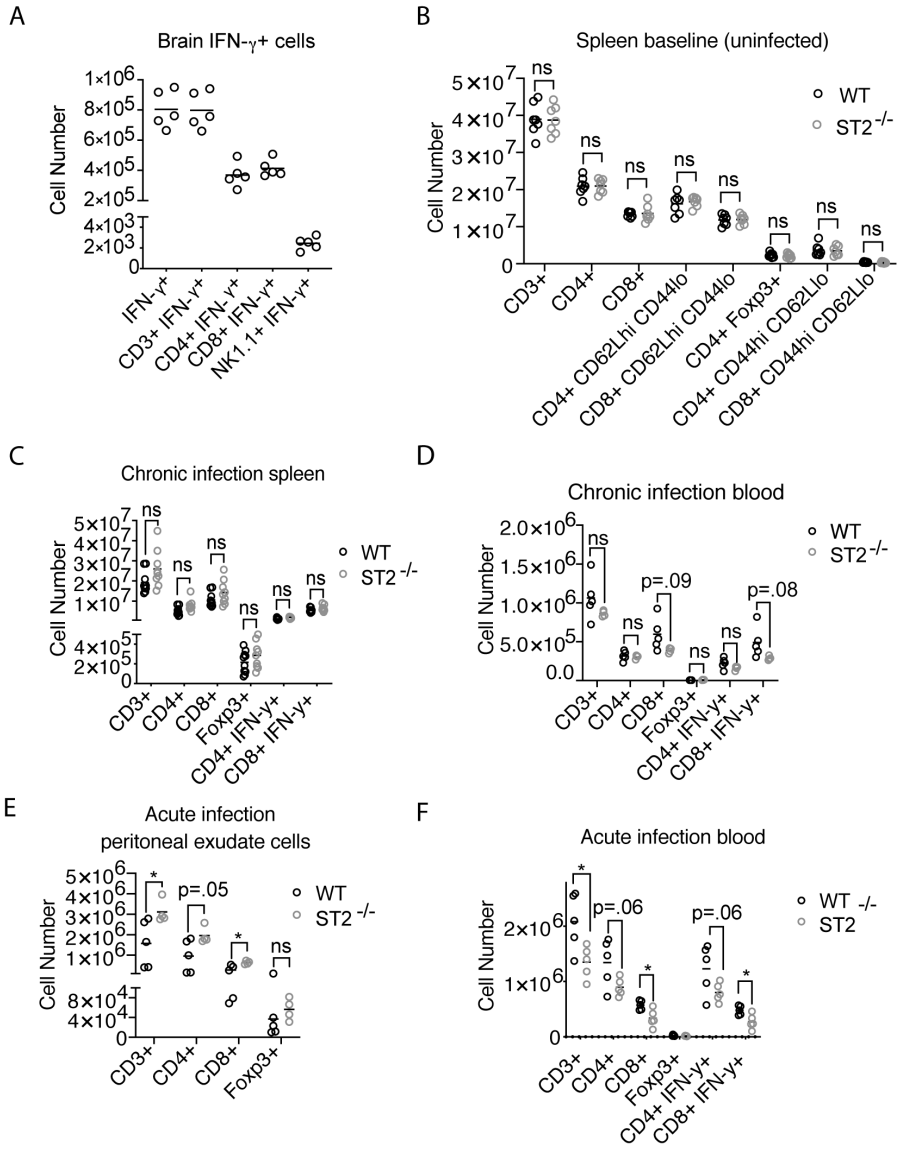

Figure S3. T cells in peripheral tissues and during acute infection in the absence of IL-33-ST2 signaling. (A) Breakdown of total IFN-γ+ cells by cell type by flow cytometry in infected brain tissue four weeks post infection. IFN-γ was measured following stimulation *ex vivo* for five hours with PMA/ionomycin. **(B)** Assessment of spleen T cell numbers in ST2-deficient mice prior to infection by flow cytometry. **(C and D)** assessment of peripheral tissue T cell numbers and activation, including spleen (C) and blood (D) by flow cytometry 4 weeks post infection. **(E and F)** T cell numbers at day 10 acute infection by flow cytometry in the peritoneum (E) and blood (F). Statistical significance was determined by randomized block ANOVA

856 when two experiments were pooled (B and C), or by two-tailed t-test (D, E, F) *= $p<.05$, **= $p<.01$, ***=

857 $p<.001$.

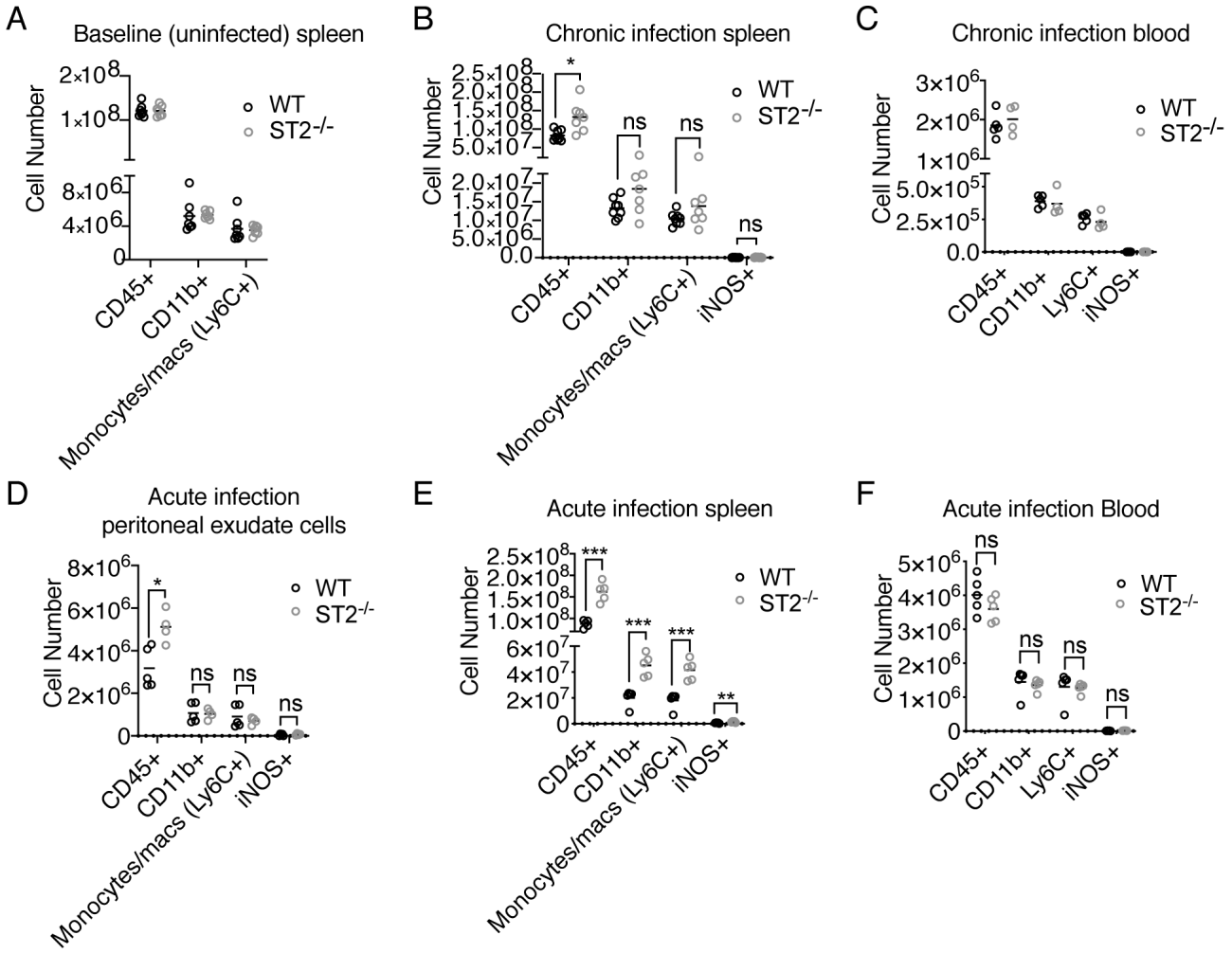

858

859 **Figure S4. The myeloid cell response is intact in peripheral tissues and during acute infection in the**
860 **absence of IL-33-ST2 signaling (A)** Assessment of spleen myeloid cell numbers in ST2-deficient mice
861 prior to infection by flow cytometry. **(B** and **C)** assessment of peripheral tissue myeloid cell numbers and
862 activation, including spleen (B) and blood (C) by flow cytometry 4 weeks post infection. **(D-F)** Myeloid
863 numbers at day 10 during acute infection by flow cytometry in the peritoneum (D), spleen (E) and blood (F).
864 Statistical significance was determined by randomized block ANOVA when two experiments were pooled
865 (A and B), or by two-tailed t-test (C-F) *= p<.05, **= p<.01, ***= p<.001.

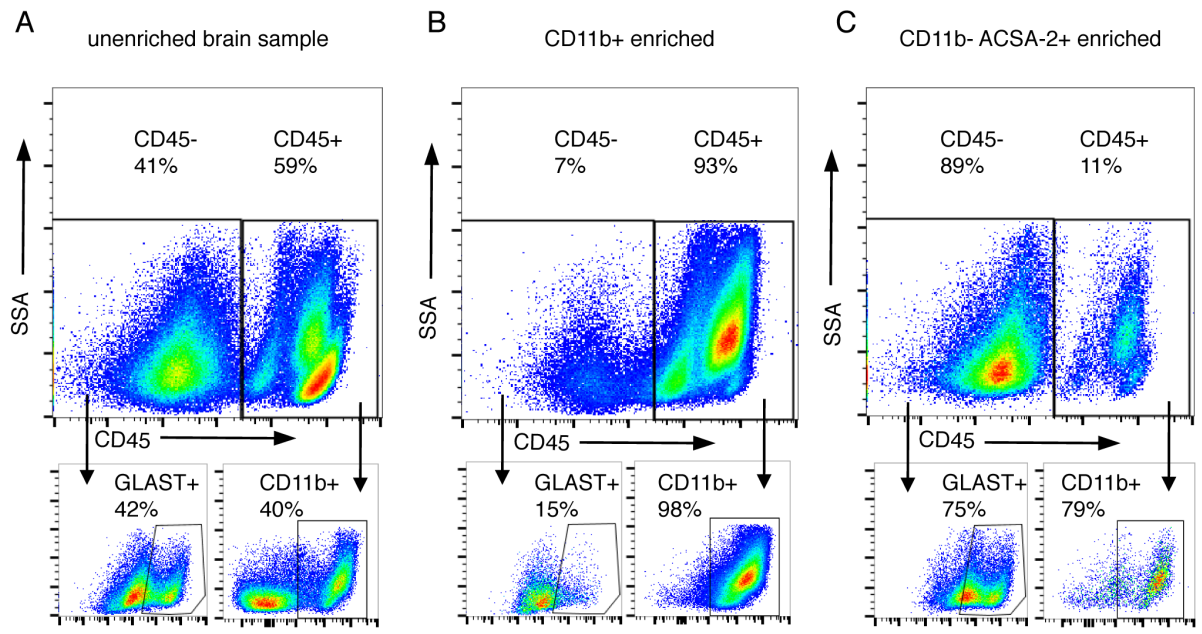

Figure S5. Magnetic enrichment for myeloid cells or astrocytes from infected brains. (A) Unenriched single cell suspension of all purified cells from infected brain tissue 4 weeks post infection. **(B and C)** Assessment of purity achieved by enriching for myeloid cells using CD11b+ magnetic beads (B), or astrocytes (C), by negatively selecting for myeloid cells using CD11b+ magnetic beads, followed by positive selection for astrocytes with ACSA-2+ magnetic beads.

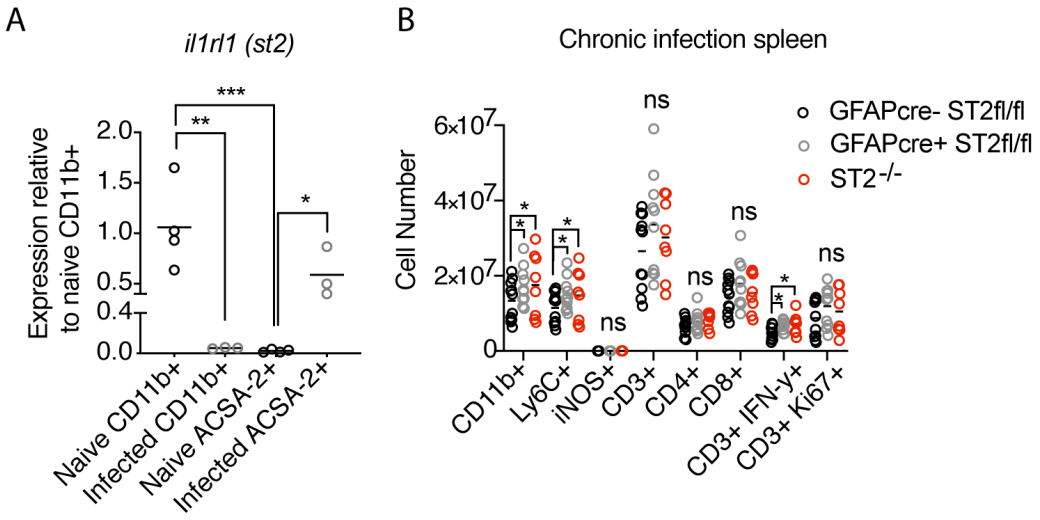

Figure S6. Astrocyte ST2 expression with infection, and astrocytic ST2-dependence for peripheral immune cell numbers (A) Cell-type specific magnetic enrichment for myeloid cells (CD11b+) or astrocytes (CD11b- and ACSA-2+) in naïve and chronically infected brain tissue. Single cell suspensions of enriched cells were resuspended in Trizol, RNA extracted, and measured by real time PCR for *ilrl1*(st2) expression. **(B)** Assessment of spleen immune cell numbers by flow cytometry four weeks post infection. Statistical significance was determined by one-way ANOVA with Tukey's test (A), or randomized block ANOVA (B) *= p<.05, **= p<.01, ***= p<.001.